Robust Control of Flexible Space Vehicles with Minimum Structural Excitation

P.89

Final Report of the First-Year Project

ON-OFF PULSE CONTROL OF FLEXIBLE SPACE VEHICLES

Bong Wie
Qiang Liu

Arizona State University

February 21, 1992

Cooperative Agreement NCC 9-16
Research Activity No. MS.05

NASA Johnson Space Center
Engineering Directorate
Navigation Control and Aeronautics Division

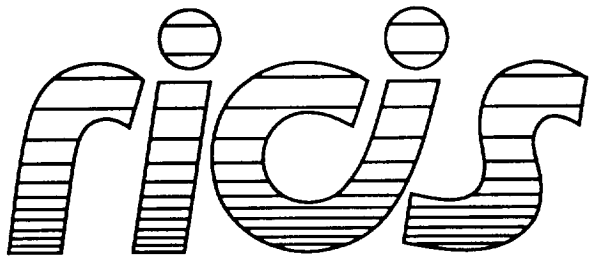

Research Institute for Computing and Information Systems
University of Houston-Clear Lake

TECHNICAL REPORT

The RICIS Concept

The University of Houston-Clear Lake established the Research Institute for Computing and Information Systems (RICIS) in 1986 to encourage the NASA Johnson Space Center (JSC) and local industry to actively support research in the computing and information sciences. As part of this endeavor, UHCL proposed a partnership with JSC to jointly define and manage an integrated program of research in advanced data processing technology needed for JSC's main missions, including administrative, engineering and science responsibilities. JSC agreed and entered into a continuing cooperative agreement with UHCL beginning in May 1986, to jointly plan and execute such research through RICIS. Additionally, under Cooperative Agreement NCC 9-16, computing and educational facilities are shared by the two institutions to conduct the research.

The UHCL/RICIS mission is to conduct, coordinate, and disseminate research and professional level education in computing and information systems to serve the needs of the government, industry, community and academia. RICIS combines resources of UHCL and its gateway affiliates to research and develop materials, prototypes and publications on topics of mutual interest to its sponsors and researchers. Within UHCL, the mission is being implemented through interdisciplinary involvement of faculty and students from each of the four schools: Business and Public Administration, Education, Human Sciences and Humanities, and Natural and Applied Sciences. RICIS also collaborates with industry in a companion program. This program is focused on serving the research and advanced development needs of industry.

Moreover, UHCL established relationships with other universities and research organizations, having common research interests, to provide additional sources of expertise to conduct needed research. For example, UHCL has entered into a special partnership with Texas A&M University to help oversee RICIS research and education programs, while other research organizations are involved via the "gateway" concept.

A major role of RICIS then is to find the best match of sponsors, researchers and research objectives to advance knowledge in the computing and information sciences. RICIS, working jointly with its sponsors, advises on research needs, recommends principals for conducting the research, provides technical and administrative support to coordinate the research and integrates technical results into the goals of UHCL, NASA/JSC and industry.

Robust Control of Flexible Space Vehicles with Minimum Structural Excitation

Final Report of the First-Year Project

ON-OFF PULSE CONTROL OF FLEXIBLE SPACE VEHICLES

Preface

This research was conducted under auspices of the Research Institute for Computing and Information Systems by Bong Wie of Arizona State University. Dr. Glen Houston served as RICIS research coordinator.

Funding has been provided by the Engineering Directorate, NASA/JSC through Cooperative Agreement NCC 9-16 between the NASA Johnson Space Center and the University of Houston-Clear Lake. Kenneth J. Cox was the Division Chief of the Navigation Control and Aeronautics Division. The NASA technical monitor for this activity was John W. Sunkel, of the Navigation Control and Aeronautics Division, Engineering Directorate, NASA/JSC.

The views and conclusions contained in this report are those of the authors and should not be interpreted as representative of the official policies, either express or implied, of NASA or the United States Government.

Final Report of the First-Year Project
Contract Number: RICIS MS 05

February 21, 1992

On-Off Pulse Control of Flexible Space Vehicles

Bong Wie and Qiang Liu
Dept. of Mechanical & Aerospace Engineering
Arizona State University
Tempe, AZ 85287-6106
(602) 965-8674

Prepared for

Dr. Kenneth Cox and Dr. John Sunkel
NASA Johnson Space Center
Houston, Texas 77058

Submitted to

RICIS
University of Houston - Clear Lake
2700 Bay Area Blvd
Houston, Texas 77058-1098

Summary

This final report documents the first-year research efforts for developing on-off pulse control techniques for flexible space vehicles which are sometimes required to maneuevr as quickly as possible with a minimum of structural vibrations during and/or a maneuver, particularly, in the presence of structural mode uncertainty.

The study objective was to explore the feasibility of computing open-loop, on-off pulse control logic for uncertain flexible spacecraft. The results indicate that the proposed *robustification* or *desensitization* approach does generate robust on-off pulse sequences for uncertain flexible spacecraft.

On the contrary to a common notion, the results show that properly coordinated, on-off pulse sequences can achieve a fast maneuvering time with a minimum of structural vibrations during and/or after a maneuver, even in the face of spacecraft modeling uncertainty. The time-optimal responses have been desensitized at the expense of the increased maneuvering time. However, it is emphasized that simply prolonging the maneuver time does not help to reduce residual structural vibrations caused by modeling uncertainty; *a proper coordination of pulse sequences is necessary.*

Acknowledgments

This research was supported by the NASA Johnson Space Center through the RICIS program of the University of Houston at Clear Lake. The authors would like to express special thanks to Dr. Kenneth Cox and Dr. John Sunkel of the NASA JSC for sponsoring this research.

Contents

A Comparison between Robustified Feedforward and Feedback Control for Performance Robustness

Bong Wie* and Qiang Liu†
Arizona State University
Tempe, Arizona

Abstract

Both feedforward and feedback control approaches for uncertain dynamical systems (in particular, with uncertainty in structural mode frequency) are investigated. The control objective is to achieve a fast settling time (high performance) and robustness (insensitivity) to plant uncertainty. Preshaping of an ideal, time-optimal control input using a *tapped-delay* filter is shown to provide a fast settling time with robust performance. A robust, non-minimum-phase feedback controller is synthesized with particular emphasis on its proper implementation for a non-zero set-point control problem. It is shown that a properly designed, feedback controller performs well, as compared with a time-optimal open-loop controller with special preshaping for performance robustness.

*Associate Professor, Dept. of Mechanical and Aerospace Engineering, Associate Fellow AIAA.
†Graduate Research Assistant, Student Member AIAA.

1. Introduction

Flexible structures, including robot manipulators and optical pointing systems in space, are sometimes required to reorient or reposition as quickly as possible with a minimum of residual structural vibrations. The control task for such systems becomes more difficult if they have many flexible modes within the rigid-body control bandwidth. The rapid maneuvering control problem of flexible dynamical systems has been investigated by many researchers, and various feedforward/feedback approaches for minimizing residual structural vibrations have been developed (e.g, see [1-9]).

The basic idea behind the various feedforward approaches is to find an input forcing function (e.g, such as a versine function) which begins and ends with zero slope so that structural modes are less likely to be excited. Such an input function, however, does not fully utilize the available maximum maneuvering force, and results in a slower response time and also residual structural vibrations. Most feedforward approaches (in particular, an open-loop optimal approach) require accurate modeling of the system and thus are not robust to plant modeling uncertainty. Recently, Singer and Seering [7-8] have developed an alternative, robust approach of shaping a feedforward input command by acausally filtering out the frequency components of flexible mode resonances. Some tradeoffs, however, must be made between performance (a fast settling time) and robustness (insensitivity) to plant parameter uncertainty even for this preshaped open-loop approach.

This paper provides a comparison between a preshaped feedforward command generator [7-8] and a robustified feedback controller [10-13] with non-zero set-point command for a reference-input tracking problem. It is, however, emphasized that one of the primary motivations for the use of closed-loop rather than open-loop control systems in practice is to cope with unexpected disturbances, which an open-loop controller cannot. Such a disturbance rejection problem is not considered in this paper. A simple generic model of uncertain dynamical systems shown in Fig. 1 is used to illustrate the control concepts and methodologies.

The remainder of this paper is organized as follows. In Section 2, time-optimal control inputs are determined for this example problem. In Section 3, such time-optimal control inputs are preshaped using a tapped-delay filter to provide a rapid

maneuver and robust suppression of residual structural vibrations. A robust H_∞ compensator design is discussed in Section 4, with special emphasis on a proper implementation of a non-minimum-phase compensator for a non-zero set-point control problem. It will be shown that a properly designed, feedback controller performs well, as compared with a time-optimal open-loop controller with special preshaping for parameter robustness.

2. Time-Optimal Control

Consider a generic example of flexible dynamical systems as shown in Fig. 1. It is assumed that the two bodies both have nominal unit mass ($m_1 = m_2 = 1$) and are connected by a spring with nominal stiffness $k = 1$. A control input force u acts on body 1 and the position of body 2 is the output to be controlled ($y = x_2$). It is assumed that the control input is bounded as $|u| \leq 1$.

In this section, time-optimal, open-loop control input $u(t)$ is determined by minimizing the performance index

$$J = \int_0^{t_f} dt = t_f. \tag{1}$$

where t_f is the final time to be obtained. The resulting time-optimal control input will be preshaped in Section 3, using a tapped-delay filter, to improve peformance robustness with respect to plant parameter uncertainty.

Rigid-Body Time-Optimal Control

For a "rigidized" model of the nominal system shown in Fig. 1, the equation of motion is simply

$$(m_1 + m_2)\ddot{y} = u. \tag{2}$$

The rest-to-rest, time-optimal solution for $y(0) = 0$ and $y(t_f) = 1$ can be found as

$$u(t) = u_s(t) - 2u_s(t - \frac{t_f}{2}) + u_s(t - t_f) \tag{3}$$

where $t_f = 2\sqrt{(m_1 + m_2)y(t_f)} = 2.828$ sec and $u_s(t)$ represents a unit-step function.

If this time-optimal input force is exerted on the nominal system with a flexible mode (Fig. 1), a significant residual structural vibration will occur, as can be seen in Fig. 2.

Flexible-Body Time-Optimal Control

Consider a time-optimal control problem for the flexible-body model shown in Fig. 1. The equations of motion are

$$m_1\ddot{x}_1 + k(x_1 - x_2) = u \tag{4a}$$

$$m_2\ddot{x}_2 - k(x_1 - x_2) = 0 \tag{4b}$$

where x_1 and x_2 are the positions of body 1 and body 2, respectively. This system can also be represented in state-space form as

$$\dot{x}(t) = Ax(t) + Bu(t) \tag{5a}$$

$$y(t) = Cx(t) \tag{5b}$$

where

$$x = \begin{bmatrix} x_1 & x_2 & x_3 & x_4 \end{bmatrix}^T$$

$$A = \begin{bmatrix} 0 & 0 & 1 & 0 \\ 0 & 0 & 0 & 1 \\ -k/m_1 & k/m_1 & 0 & 0 \\ k/m_2 & -k/m_2 & 0 & 0 \end{bmatrix}, \qquad B = \begin{bmatrix} 0 \\ 0 \\ 1/m_1 \\ 0 \end{bmatrix},$$

$$C = \begin{bmatrix} 0 & 1 & 0 & 0 \end{bmatrix}.$$

The time-optimal control input for this problem, which first appeared in [10], can be solved using the following approach discussed in [4]. For our two-mass-spring model, three switching times are required. The nominal system with $m_1 = m_2 = k = 1$ is first transformed into modal equations by the coordinate transformation

$$\begin{bmatrix} x_1 \\ x_2 \end{bmatrix} = \begin{bmatrix} 1 & 1 \\ 1 & -1 \end{bmatrix} \begin{bmatrix} q_1 \\ q_2 \end{bmatrix} \tag{6}$$

where q_1 and q_2 are the modal coordinates, and the resulting modal equations are

$$\ddot{q}_1 = u/2 \tag{7a}$$

$$\ddot{q}_2 + \omega^2 q_2 = u/2 \tag{7b}$$

where $\omega = \sqrt{2}$ rad/sec is the nominal flexible mode frequency. For given boundary conditions

$$\begin{aligned} q_1(0) = 0, \quad \dot{q}_1(0) = 0, \\ q_2(0) = 0, \quad \dot{q}_2(0) = 0, \\ q_1(t_f) = 1, \quad \dot{q}_1(t_f) = 0, \\ q_2(t_f) = 0, \quad \dot{q}_2(t_f) = 0, \end{aligned}$$

the following two constraint equations can be obtained as

$$\begin{aligned} 1 - 2cos\omega t_1 + 2cos\omega t_2 - 2cos\omega t_3 + cos\omega t_f = 0 \\ 4 - t_f^2 + 2(t_f - t_1)^2 - 2(t_f - t_2)^2 + 2(t_f - t_3)^2 = 0 \end{aligned}$$

where t_1, t_2, and t_3 are the switching times and t_f the final time to be solved. From the symmetric nature of this problem, we have

$$\begin{aligned} t_2 = t_f/2 \\ t_1 = t_f - t_3, \end{aligned}$$

and the switching times can be found as

$$t_1 = 1.00268 \ \text{sec}$$

$$\begin{aligned} t_2 = 2.10893 \ \text{sec} \\ t_3 = 3.21518 \ \text{sec} \\ t_f = 4.21786 \ \text{sec}. \end{aligned}$$

Note that a longer maneuver time of 4.217 sec is required for a flexible body, as compared with the maneuver time of 2.828 sec for a rigidized system.

The time-optimal control input can then be expressed as

$$\begin{aligned} u(t) = u_s(t) - 2u_s(t - t_1) + 2u_s(t - t_2) \\ - 2u_s(t - t_3) + u_s(t - t_f). \end{aligned} \tag{8}$$

The open-loop responses of the system to this time-optimal control input are shown in Fig. 3 for four different values of k. It can be seen that an ideal, minimum-time maneuver is achieved for the nominal system and that perturbations in spring constant k, however, result in residual vibrations of the flexible mode.

3. Preshaped Time-Optimal Control

As shown in the preceding section, the time-optimal solution requires accurate modeling of the system, and the open-loop responses to such an ideal input force are very sensitive to the plant modeling uncertainty. In this section, an "impulse-sequence" shaping technique developed by Singer and Seering [7-8] is employed to preshape the ideal, time-optimal inputs. Performance of the resulting robust feedforward controller will be compared with that of a robust, feedback controller in Section 4.

The preshaping technique in [7-8] simply utilizes a tapped-delay filter with proper weightings and time delays. This technique is briefly reviewed here for our example with a single, undamped flexible mode.

A sequence of m impulses can be expressed in time domain as

$$f(t) = \sum_{i=1}^{m} A_i \delta(t - t_i) \tag{9}$$

with the following normalization

$$\sum_{i=1}^{m} A_i = 1 \tag{10}$$

where A_i is the magnitude of the i^{th} impulse at $t = t_i$ and the last impulse occurs at $t = t_m$.

A bang-bang function with $(n-2)$ switches can be represented as

$$u(t) = \sum_{j=1}^{n} B_j u_s(t - t_j) \tag{11}$$

where B_j is the magnitude of a step function at $t = t_j$. This bang-bang function ends at $t = t_n$.

The convolution of $u(t)$ and $f(t)$ will result in a new multi-switch, multi-level, bang-bang function

$$\tilde{u}(t) = \sum_{i=1}^{n}\sum_{j=1}^{m} A_i B_j u_s(t - t_i - t_j). \tag{12}$$

This function has $(mn-2)$ switching times and ends at $t = (t_m + t_n)$.

A proper sequence of impulses, whose power spectrum has a notch at a structural resonant frequency, can be found as follows. If a sequence of m impulses in Eq. (9) is applied to an undamped second-order system with natural frequency of ω, the system response for $t > t_m$ can be represented as:

$$\sum_{i=1}^{m} A_i \omega sin\omega(t - t_i) = Asin(\omega t - \phi) \tag{13}$$

where

$$A = \sqrt{(\sum_{i=1}^{m} A_i \omega cos\omega t_i)^2 + (\sum_{i=1}^{m} A_i \omega sin\omega t_i)^2}$$

$$\phi = tan^{-1}(\frac{\sum_{i=1}^{m} A_i sin\omega t_i}{\sum_{i=1}^{m} A_i cos\omega t_i}).$$

If A_i's and t_i's are chosen such that $A = 0$, that is,

$$A_1 cos\omega t_1 + A_2 cos\omega t_2 + \cdots + A_m cos\omega t_m = 0 \tag{14a}$$

$$A_1 sin\omega t_1 + A_2 sin\omega t_2 + \cdots + A_m sin\omega t_m = 0 \tag{14b}$$

then the residual vibration will not occur after $t = t_m$.

Taking derivatives of the preceding two equations for $(m-2)$ times with respect to ω, we get the following $2(m-2)$ robustness constraint equations

$$A_1(t_1)^j sin\omega t_1 + A_2(t_2)^j sin\omega t_2 + \cdots + A_m(t_m)^j sin\omega t_m = 0 \tag{15a}$$

$$A_1(t_1)^j cos\omega t_1 + A_2(t_2)^j cos\omega t_2 + \cdots + A_m(t_m)^j cos\omega t_m = 0 \tag{15b}$$

$$j = 1, \cdots, m-2 \ .$$

For an m-impulse sequence with $t_1 = 0$, we now have $(2m-1)$ equations for $(2m-1)$ unknowns.

Figure 4 illustrates three different impulse-sequences with proper A_i's and the time-delay interval of $\Delta T = \pi/\omega$, where ω is the natural frequency of the flexible mode under consideration.

The frequency response characteristics of this impulse-sequence shaping technique can be analyzed simply by taking the Laplace transform of an m-impulse sequence as follows:

$$\begin{aligned} \mathrm{L}[f(t)] &= \sum_{i=1}^{m} A_i e^{-t_i s} \\ &= \sum_{i=1}^{m} A_i e^{-\Delta T(i-1)s} \end{aligned} \tag{16}$$

which can be interpreted as a tapped-delay filter (see Fig. 5). The frequency responses of this tapped-delay filter for $m = 2$, 3 and 4 are shown in Fig. 6. It can be seen that the frequency component around the resonant frequency is notched out. The wider notch width indicates more robustness to frequency uncertainty, but a longer response time.

The flexible-body time-optimal input given by Eq. 8 is now preshaped by a tapped-delay filter with $m = 2$, resulting in the preshaped input command

$$\begin{aligned} \tilde{u}(t) = {} & 0.5u_s(t) - u_s(t - 1.003) + u_s(t - 2.109) \\ & + 0.5u_s(t - 2.221) - u_s(t - 3.215) \\ & - u_s(t - 3.224) + 0.5u_s(t - 4.218) \\ & + u_s(t - 4.330) - u_s(t - 5.436) \\ & + 0.5u_s(t - 6.439). \end{aligned} \tag{17}$$

This preshaped input takes values of ± 1.0 and ± 0.5.

The flexible-body time-optimal input is also preshaped using a tapped-delay filter with $m = 3$, resulting in the preshaped control input command

$$\begin{aligned} \tilde{u}(t) = {} & 0.25u_s(t) - 0.5u_s(t - 1.003) + 0.5u_s(t - 2.109) \\ & + 0.5u_s(t - 2.221) - 0.5u_s(t - 3.215) \\ & - u_s(t - 3.224) + 0.25u_s(t - 4.218) \end{aligned}$$

$$
\begin{aligned}
&+ u_s(t - 4.330) + 0.25u_s(t - 4.442) \\
&- u_s(t - 5.436) - 0.5u_s(t - 5.445) \\
&+ 0.5u_s(t - 6.439) + 0.5u_s(t - 6.551) \\
&- 0.5u_s(t - 7.657) + 0.25u_s(t - 8.660).
\end{aligned} \tag{18}
$$

It can be seen from Fig. 7 that the preshaped command takes values of ± 0.25, ± 0.5 and ± 0.75. The time responses of the system to this preshaped input are shown in Fig. 8 for four different values of k. It is evident that robustness with respect to flexible mode frequency has been increased at the expense of increasing manuever time to about 8.66 sec, comparing with the ideal minimum time of 4.218 sec shown in Fig. 3.

The simple, rigid-body time-optimal input given by Eq. 3 can also be preshaped to reduce the residual vibration shown in Fig. 2. For example, preshaping the rigid-body bang- bang command with a tapped-delay filter with $m = 3$ results in another bang- bang command:

$$
\begin{aligned}
u(t) = {} & 0.25u_s(t) - 0.5u_s(t - 1.414) + 0.5u_s(t - 2.221) \\
& + 0.25u_s(t - 2.828) - u_s(t - 3.635) \\
& + 0.25u_s(t - 4.442) + 0.5u_s(t - 5.049) \\
& - 0.5u_s(t - 5.856) + 0.25u_s(t - 7.270).
\end{aligned} \tag{19}
$$

The responses of the system to this preshaped input (not shown here) also indicate a reasonable performance robustness (but not better than Fig. 8). In practice, however, the time-optimal solution for a rigidized rather than flexible model of a multi-link flexible robot (e.g, see [14]) may be preshaped using a tapped-delay filter to accommodate the flexible mode effects.

In summary, we have shown that time-optimal control input, preshaped using a tapped delay filter, provides a robust maneuvering scheme which can minimize residual structural vibrations. It is also evident that some tradeoffs between performance and robustness must always be considered. In the next section, a robust feedback compensator will be designed and its performance and robustness will be compared with that of the robust, preshaped feedforward approach discussed in this section.

4. Robust Feedback Control Design

As discovered in [10-13], a non-minimum-phase compensation is particularly useful for practical tradeoffs between performance and robustness for a certain class of noncolocated structural control problems. It is, however, often criticized because of its sluggish response and its loop gain limitation. In this section, a robust H_∞ feedback compensator design is discussed with special emphasis on a proper implementation of a non-minimum-phase compensator, incorporating a non-zero set-point control scheme. It is shown that a properly designed, feedback controller with a non-zero set-point command performs well, as compared with a time-optimal, open-loop controller with special preshaping for robustness.

Consider a single-input single-output (SISO) control system as illustrated in Fig. 9, which is the most commonly used configuration for a "two-degree-of-freedom" controller. The plant and compensator transfer functions are represented as

$$K(s) = \frac{N_c(s)}{D_c(s)} \tag{20a}$$

$$G(s) = \frac{N(s)}{D(s)} \tag{20b}$$

where $N_c(s)$, $D_c(s)$, $N(s)$ and $D(s)$ are polynomials of the Laplace transform variable s. The closed-loop transfer function from the desired output command y^* to the actual output y is then

$$\begin{aligned} \frac{y(s)}{y^*(s)} &= \frac{K(s)G(s)}{1 + K(s)G(s)} F(s) \\ &= \frac{N_c N}{D_c D + N_c N} F(s). \end{aligned} \tag{21}$$

Thus, for the conventional feedback control system of Fig. 9, the zeros of the closed-loop transfer function are identical with the zeros of the loop transfer function $K(s)G(s)$. These zeros sometimes cause an excessive, transient peak overshoot even when the closed-loop poles are properly selected. In this case, a prefilter $F(s)$ is often used for the cancellation of the undesirable zeros of the closed-loop transfer function. (Of course, we cannot cancel the non-minimum-phase zeros!)

If the compensator is placed in the feedback path, the closed-loop transfer function becomes

$$\begin{aligned}\frac{y(s)}{y^*(s)} &= \frac{G(s)}{1+K(s)G(s)}F(s) \\ &= \frac{D_c N}{D_c D + N_c N}F(s)\end{aligned} \tag{22}$$

where the compensator zeros do not appear as zeros of the closed-loop transfer function, and a prefilter $F(s)$ must be properly designed for the generation of a control input command. Recall that one of the primary motivations for the use of closed-loop rather than open-loop control systems in practice is to cope with unexpected disturbances, which an open-loop controller cannot. For this reason, feedforward control is seldom used alone, but rather, it is used in combination with feedback control.

In this section, we show a proper way of implementating a non-minimum-phase compensator to minimize such excessive, transient peak overshoot caused by the compensator zeros. We briefly review a robust H_∞ control design methodology developed in [12-13], and we present a non-zero set-point control scheme for an H_∞-based controller, followed by an example design.

Robust H_∞ Control

Consider a linear, time-invariant system described by [15]

$$\begin{aligned}\dot{x}(t) &= Ax(t) + B_1 w(t) + B_2 u(t) \\ z(t) &= C_1 x(t) + D_{11} w(t) + D_{12} u(t) \\ y(t) &= C_2 x(t) + D_{21} w(t) + D_{22} u(t)\end{aligned} \tag{23}$$

where $x(t)$ is an n-dimensional state vector, $w(t)$ an m_1-dimensional disturbance vector, $u(t)$ an m_2-dimensional control vector, $z(t)$ a p_1-dimensional controlled output vector, and $y(t)$ a p_2-dimensional measurement vector.

In order to utilize the concept of an internal feedback loop, the system with uncertain parameters is described as [12, 13]

$$\begin{bmatrix} \dot{x} \\ z \\ y \end{bmatrix} = \begin{bmatrix} \hat{A} & \hat{B}_1 & \hat{B}_2 \\ C_1 & D_{11} & D_{12} \\ \hat{C}_2 & \hat{D}_{21} & \hat{D}_{22} \end{bmatrix} \begin{bmatrix} x \\ w \\ u \end{bmatrix} \tag{24}$$

where C_1, D_{11}, and D_{12} are not subject to parameter variations. The perturbed system matrix in Eq. (24) can be linearly decomposed as follows:

$$\begin{bmatrix} \dot{x} \\ z \\ y \end{bmatrix} = \left\{ \begin{bmatrix} A & B_1 & B_2 \\ C_1 & D_{11} & D_{12} \\ C_2 & D_{21} & D_{22} \end{bmatrix} + \Delta_p \right\} \begin{bmatrix} x \\ w \\ u \end{bmatrix} \tag{25}$$

where the first matrix in the right-hand side is the nominal system matrix and Δ_p is the perturbation matrix defined as

$$\Delta_p \triangleq \begin{bmatrix} \Delta A & \Delta B_1 & \Delta B_2 \\ 0 & 0 & 0 \\ \Delta C_2 & \Delta D_{21} & \Delta D_{22} \end{bmatrix}. \tag{26}$$

Suppose that there are l independent perturbed parameters $p_1, \ldots, p_l$ which are bounded as $|\Delta p_i| \leq 1$. The perturbation matrix Δ_p is then decomposed with respect to each parameter variation as

$$\Delta_p = - \begin{bmatrix} M_x \\ 0 \\ M_y \end{bmatrix} E \begin{bmatrix} N_x & N_w & N_u \end{bmatrix} = -MEN \tag{27}$$

where

$$E = \begin{bmatrix} \Delta p_1 & & 0 \\ & \ddots & \\ 0 & & \Delta p_l \end{bmatrix}. \tag{28}$$

By introducing the following new variables

$$z_p \triangleq \begin{bmatrix} N_x & 0 & N_w & N_u \end{bmatrix} \begin{bmatrix} x \\ w_p \\ w \\ u \end{bmatrix} \tag{29a}$$

$$w_p \triangleq -E z_p, \tag{29b}$$

the perturbed system, Eq. (25), and the input-output decomposition, Eq. (27), can be combined as:

$$\begin{bmatrix} \dot{x} \\ z_p \\ z \\ y \end{bmatrix} = \begin{bmatrix} A & M_x & B_1 & B_2 \\ N_x & 0 & N_w & N_u \\ C_1 & 0 & D_{11} & D_{12} \\ C_2 & M_y & D_{21} & D_{22} \end{bmatrix} \begin{bmatrix} x \\ w_p \\ w \\ u \end{bmatrix} \tag{30a}$$

$$w_p = -E z_p \tag{30b}$$

where w_p and z_p are considered as the fictitious input and output, respectively, due to the plant perturbation; and E is considered as a fictitious, internal feedback loop gain matrix.

The following redefinition of z, w, and expansion of the associated matrices enable us to employ the state-space representation given by Eq. (23):

$$\begin{aligned} z &\leftarrow \begin{bmatrix} z_p \\ z \end{bmatrix}, & w &\leftarrow \begin{bmatrix} w_p \\ w \end{bmatrix} \\ B_1 &\leftarrow \begin{bmatrix} M_x & B_1 \end{bmatrix}, & C_1 &\leftarrow \begin{bmatrix} N_x \\ C_1 \end{bmatrix} \\ D_{11} &\leftarrow \begin{bmatrix} 0 & N_w \\ 0 & D_{11} \end{bmatrix}, & D_{12} &\leftarrow \begin{bmatrix} N_u \\ D_{12} \end{bmatrix} \\ D_{21} &\leftarrow \begin{bmatrix} M_y & D_{21} \end{bmatrix} \end{aligned} \qquad (31)$$

It can be shown that under certain conditions, there exists an internally stabilizing controller such that, for the closed-loop transfer matrix T and for a given design variable γ,

$$\|T\|_\infty < \gamma$$

if and only if the following Riccati equations [15]

$$0 = A^T X + XA - X(B_2 B_2^T - \frac{1}{\gamma^2} B_1 B_1^T)X + C_1^T C_1 \qquad (32)$$

$$0 = AY + YA^T - Y(C_2^T C_2 - \frac{1}{\gamma^2} C_1^T C_1)Y + B_1 B_1^T \qquad (33)$$

have unique symmetric positive semi-definite solutions X and Y.

An H_∞-suboptimal controller that satisfies $\|T_{zw}\|_\infty < \gamma$, where γ is a design variable specifying an upper bound of the perturbed closed-loop performance T_{zw}, is then obtained as

$$u(s) = -K[sI - A_c]^{-1} L y(s) \qquad (34)$$

or

$$\dot{x}_c = A_c x_c + Ly \qquad (35a)$$

$$u = -Kx_c \qquad (35b)$$

where

$$K = B_2^T X \tag{36a}$$

$$L = (I - \frac{1}{\gamma^2} YX)^{-1} YC_2^T \tag{36b}$$

$$A_c = A + \frac{1}{\gamma^2} B_1 B_1^T X - B_2 K - LC_2. \tag{36c}$$

Note that this H_∞ controller has a structure similar to a conventional state-space controller consisting of an estimator and a regulator, but is designed for a plant system matrix

$$A + \frac{1}{\gamma^2} B_1 B_1^T X$$

where $B_1 B_1^T X/\gamma^2$ can be interpreted as an estimate for the worst disturbance input. In other words, the separation principle of the conventional linear-quadratic-gaussian (LQG) technique does not hold here. Consequently, the non-zero set-point control scheme, which has been well established for LQG control synthesis, needs some minor modification as discussed in the next section.

Non-Zero Set-Point Control

A block diagram representation of a SISO closed-loop system for a conventional LQG-type controller with a non-zero set-point command is illustrated in Fig. 10. For this configuration, the control input command, u^*, corresponding to the desired (constant) output command, y^*, is simply given as

$$u^* = -[C(A - BK)^{-1} B]^{-1} y^* \tag{37}$$

which is independent of the estimator gain matrix L. In this case, we can easily show that for dynamic systems having a rigid-body mode, u^* depends only on the regulator parameters (not on the plant parameters such as m_1, m_2, and k of the example model shown in Fig. 1). Hence, the non-zero set-point control scheme is inherently robust to plant parameter uncertainty for a certain class of dynamical systems with at least one pole at the origin (i.e., a type-1 system).

Now consider a closed-loop control system with an H_∞ controller as shown in Fig.

11, which is described in state-space form as

$$\begin{bmatrix} \dot{x} \\ \dot{x}_c \end{bmatrix} = \begin{bmatrix} A & -B_2K \\ LC_2 & A_c \end{bmatrix} \begin{bmatrix} x \\ x_c \end{bmatrix} + \begin{bmatrix} B_2 \\ B_2 \end{bmatrix} u^*$$
$$y = \begin{bmatrix} C_2 & 0 \end{bmatrix} \begin{bmatrix} x \\ x_c \end{bmatrix}. \tag{38a}$$

The input command u^* corresponding to the desired output y^* can be simply found as

$$u^* = -[\bar{C}\bar{A}^{-1}\bar{B}]^{-1}y^* \tag{39}$$

where

$$\bar{A} = \begin{bmatrix} A & -B_2K \\ LC_2 & A_c \end{bmatrix}, \quad \bar{B} = \begin{bmatrix} B_2 \\ B_2 \end{bmatrix}$$
$$\bar{C} = \begin{bmatrix} C_2 & 0 \end{bmatrix}. \tag{40}$$

Similarly to the LQG case, it can be shown that for dynamic systems having a rigid-body mode, u^* for an H_∞ controller depends only on the controller parameters (not on the plant parameters such as m_1, m_2, and k of the example model shown in Fig. 1). However, u^* now depends on both the gain matrices K and L , not just on the regulator gain matrix K as for the LQG case.

Example Design

We now consider the two-mass-spring model shown in Fig. 1. A control input force u acts on body 1 and the position of body 2 is measured as y, resulting in the so-called noncolocated control problem. The control design objective here is to achieve a fast settling time (high performance) for an output command $y^* = 1$ and robust performance over a range of spring stiffness uncertainty considered in Section 3. The control input is bounded as $|u| \leq 1$ and the system has the nominal values of $m_1 = m_2 = k = 1$.

The plant model can be represented in state-space form as:

$$\begin{bmatrix} \dot{x}_1 \\ \dot{x}_2 \\ \dot{x}_3 \\ \dot{x}_4 \end{bmatrix} = \begin{bmatrix} 0 & 0 & 1 & 0 \\ 0 & 0 & 0 & 1 \\ -k & k & 0 & 0 \\ k & -k & 0 & 0 \end{bmatrix} \begin{bmatrix} x_1 \\ x_2 \\ x_3 \\ x_4 \end{bmatrix}$$
$$+ \begin{bmatrix} 0 \\ 0 \\ 1 \\ 0 \end{bmatrix} (u + w_1) \tag{41a}$$

$$y = x_2 + v \tag{41b}$$

$$z = x_2 \tag{41c}$$

where w_1 and v are, respectively, plant disturbance and sensor noise assumed for control design purposes.

The variation ΔA is decomposed as

$$\Delta A = -\Delta k \begin{bmatrix} 0 \\ 0 \\ 1 \\ -1 \end{bmatrix} \begin{bmatrix} 1 & -1 & 0 & 0 \end{bmatrix}. \tag{42}$$

The other elements of the perturbation matrix in Eq. (26) are all zeros. Note that ΔA is spanned by the matrices

$$M_x = \begin{bmatrix} 0 \\ 0 \\ 1 \\ -1 \end{bmatrix} \quad \text{and} \quad N_x = \begin{bmatrix} 1 & -1 & 0 & 0 \end{bmatrix}$$

where M_x is the fictitious disturbance distribution matrix spanning the columns of ΔA, and N_x is the fictitious controlled output distribution matrix spanning the rows of ΔA. The fictitious input and output for this example are expressed as

$$z_p = Nx = x_1 - x_2 \quad \text{and} \quad w_p = -\Delta k\, z_p. \tag{43}$$

Equation (43) replaces the parameter variation in Eqs. (41), resulting in the following equations:

$$\begin{bmatrix} \dot{x}_1 \\ \dot{x}_2 \\ \dot{x}_3 \\ \dot{x}_4 \end{bmatrix} = \begin{bmatrix} 0 & 0 & 1 & 0 \\ 0 & 0 & 0 & 1 \\ -k & k & 0 & 0 \\ k & -k & 0 & 0 \end{bmatrix} \begin{bmatrix} x_1 \\ x_2 \\ x_3 \\ x_4 \end{bmatrix} + \begin{bmatrix} 0 \\ 0 \\ 1 \\ 0 \end{bmatrix} (u + w_1) + \begin{bmatrix} 0 \\ 0 \\ 1 \\ -1 \end{bmatrix} w_p \tag{44a}$$

$$\begin{bmatrix} z_p \\ z \end{bmatrix} = \begin{bmatrix} x_1 - x_2 \\ x_2 \\ u \end{bmatrix} \tag{44b}$$

$$y = x_2 + v \tag{44c}$$

where k is the nominal spring constant. As can be seen in Eq. (44b), control input u is also included in the performance variable z in order to minimize control effort.

By defining

$$w \leftarrow \begin{bmatrix} w_p \\ w_1 \\ v \end{bmatrix} \quad \text{and} \quad z \leftarrow \begin{bmatrix} z_p \\ z \end{bmatrix}, \tag{45}$$

and by using the definition of Eq. (31), the system matrices in Eq. (23) can be represented as

$$A = \begin{bmatrix} 0 & 0 & 1 & 0 \\ 0 & 0 & 0 & 1 \\ -k & k & 0 & 0 \\ k & -k & 0 & 0 \end{bmatrix}$$

$$B_1 = \begin{bmatrix} 0 & 0 & 0 \\ 0 & 0 & 0 \\ 1 & 1 & 0 \\ -1 & 0 & 0 \end{bmatrix}, \qquad B_2 = \begin{bmatrix} 0 \\ 0 \\ 1 \\ 0 \end{bmatrix}$$

$$C_1 = \begin{bmatrix} 1 & -1 & 0 & 0 \\ 0 & 1 & 0 & 0 \\ 0 & 0 & 0 & 0 \end{bmatrix}, \quad D_{12} = \begin{bmatrix} 0 \\ 0 \\ 1 \end{bmatrix}$$

$$C_2 = \begin{bmatrix} 0 & 1 & 0 & 0 \end{bmatrix}, \qquad D_{21} = \begin{bmatrix} 0 & 0 & 1 \end{bmatrix}$$

and $D_{11} = 0_{3\times 3}$, $D_{22} = 0$.

For the example design considered here, the disturbances w_p, w_1, and v are multiplied by weighting factors, 0.1, 0.025, and 0.025, respectively. The performance specification bound γ is chosen to be 1. The weighting factors and γ represent relative disturbance levels and overall closed-loop performance level, respectively.

By solving two Riccati equations, Eqs. (32) and (33), we get the controller gain matrices K and L as follows:

$$K = \begin{bmatrix} 1.506 & -0.494 & 1.738 & 0.932 \end{bmatrix},$$
$$L = \begin{bmatrix} 0.720 & 2.973 & -3.370 & 4.419 \end{bmatrix}^T.$$

The corresponding robust H_∞ controller is then

$$u(s) = -\frac{0.0827(\frac{s}{0.145}+1)(-\frac{s}{0.984}+1)}{[(\frac{s}{1.586})^2+2(0.825)(\frac{s}{1.586})+1]} \cdot \frac{(\frac{s}{3.434}+1)}{[(\frac{s}{2.240})^2+2(0.459)(\frac{s}{2.240})+1]} y(s) \tag{47}$$

which is a non-minimum-phase compensator.

Figure 12 shows a closed-loop root locus versus overall gain of this compensator. The gain margin is 3.28 dB, and the closed-loop system is stable for $0.44 \leq k \leq 3.27$, which corresponds to $-0.56 \leq \Delta k \leq +2.27$. The nominal system's closed-loop poles are:

$$\begin{array}{ll} -0.337 \pm 0.336j, & -0.514 \pm 0.414j, \\ -0.376 \pm 1.495j, & -1.109 \pm 1.797j. \end{array} \tag{48}$$

The time response of the closed-loop system implemented as in Fig. 9, for $F(s) = 1$ and $y^* = 1$, is shown in Fig. 13. A non-minimum-phase behavior of the closed-loop system is evident and the nominal system has a peak overshoot of about 80% and a settling time of 15 sec. When compared with the response of a feedforward controller, shown in Fig. 8, the overall response is not acceptable. It can be shown that the excessive overshoot is due to the compensator zero at $s = -0.145$. This zero may be cancelled by a prefilter $F(s)$, but the resulting slower settling time may not be desirable.

Figure 14 shows the closed-loop responses for four different values of k to an output command of $y^* = 1$ (consequently, $u^* = 0.9959$), when the same controller is implemented as in Fig. 11. Clearly, the responses no longer have excessive overshoot and the settling time is quite short, as compared with the response in Fig. 13. The overall responses are also comparable with those of a preshaped feedforward controller, as can be seen in Fig. 14. The control input $u(t)$ is always within the saturation limit of one.

In summary, we may conclude that a feedback controller, when implemented properly, could achieve good performance and robustness, for both command following as well as disturbance rejection problems. The proposed feedforward/feedback control approach is robust for a certain class of uncertain dynamical systems, since the control input command computed for a given desired output does not depend on the plant parameters.

5. Conclusions

In this paper we have investigated both feedforward and feedback control approaches for rapid maneuvering control of uncertain dynamical systems. A simple two-mass-spring example was used to illustrate the control concepts and methodologies. It was shown that a time-optimal control input, preshaped using a tapped-delay filter, provides a rapid maneuver and robust suppression of residual structural vibrations. A proper implementation of a non-minimum-phase compensator with a non-zero set-point control command was discussed. It was demonstrated that a properly implemented feedback controller performs well, when compared with a time-optimal, open-loop controller with special preshaping for performance robustness.

Acknowledgments

This research was supported by the NASA Johnson Space Center through the RICIS program at the University of Houston at Clear Lake. The authors gratefully acknowledge the technical assistance of Dr. Kenneth Cox and Dr. John Sunkel at NASA JSC and their sponsoring this research for possible applications to real space missions.

References

[1] C.J. Swigert, "Shaped Torque Techniques," *Journal of Guidance and Control*, Vol. 3, No. 5, Sept.-Oct., 1980, pp. 460–467.

[2] D.M. Aspinwall, "Acceleration Profiles for Minimizing Residual Response," *Journal of Dynamic Systems, Measurement and Control*, Vol.102, March 1980, pp. 3–7.

[3] I. Yamada and Nakagawa, "Reduction of Residual Vibrations in Positioning Control Mechanism," *Journal of Vibration, Acoustics, Stress and Reliability in Design*, Vol.107, Jan.,1985, pp. 47–52.

[4] P.H. Meckl and W.P. Seering, "Active Damping in a Three-Axis Robotic Manipulator," *Journal of Vibration, Acoustics, Stress and Reliability in Design*, Vol.107, Jan.,1985, pp. 38–46.

[5] P.H. Meckl and W.P. Seering, "Minimizing Residual Vibration for Point-to-Point Motion," *Journal of Vibration, Acoustics, Stress and Reliability in Design*, Vol.107, Oct.,1985, pp. 378–382.

[6] P.H. Meckl and W.P. Seering, "Feedforward Control Techniques to Achieve Fast Settling Time in Robots," *Proc. of the American Control Conference*, 1986, pp. 1913–1918.

[7] N.C. Singer and W.P. Seering, "Using Acausal Shaping Techniques to Reduce Robot Vibration," *Proc. of the 1988 IEEE International Conference on Robotics and Automation*, Philadelphia, PA, April 25-29, 1988.

[8] N.C. Singer and W.P. Seering, "Preshaping Command Inputs to Reduce System Vibration," *Proc. of the 1989 IEEE International Conference on Robotics and Automation*, Scottsdale, Arizona, May, 1989.

[9] R.M. Byers, S.R. Vadali and J.L. Junkins, "Near-Minimum Time, Closed-Loop Slewing of Flexible Spacecraft," *Journal of Guidance, Control and Dynamics*, Vol. 13, No. 1, 1990, pp.57-65.

[10] A.E. Bryson, Jr., S. Hermelin, and J. Sun, "LQG Controller Design for Robustness," Presented at the American Control Conference, Seattle, Washington, June, 1986.

[11] B. Wie and K.W. Byun, "New Generalized Structural Filtering Concept for Active Vibration Control Synthesis," *Journal of Guidance, Control, and Dynamics*, Vol.12, No.2, 1989, pp.147-154.

[12] K.W. Byun, B. Wie, and J. Sunkel, "Robust Control Synthesis for Uncertain Dynamical Systems," AIAA Paper No. 89-3516, to appear in the *Journal of Guidance, Control, and Dynamics.*

[13] B. Wie, Q. Liu and and K.-W. Byun, "Robust H_∞ Control Design Method and Its Application to a Benchmark Problem," presented at the 1990 American Control Conference, San Diego, CA, May 1990, to appear in the *Journal of Guidance, Control, and Dynamics.*

[14] B. Wie, C.-H. Chuang and J. Sunkel, "Minimum-Time Pointing Control of a Two-Link Manipulator," *Journal of Guidance, Control and Dynamics*, Vol. 13, No. 5, 1990, pp. 867-873.

[15] J. Doyle, K. Glover, P. Khargonekar, and B. Francis, "State-Space Solutions to Standard H_2 and H_∞ Control Problems," *IEEE Trans. Automatic Control*, Vol.34, No.8, 1989, pp.831-847.

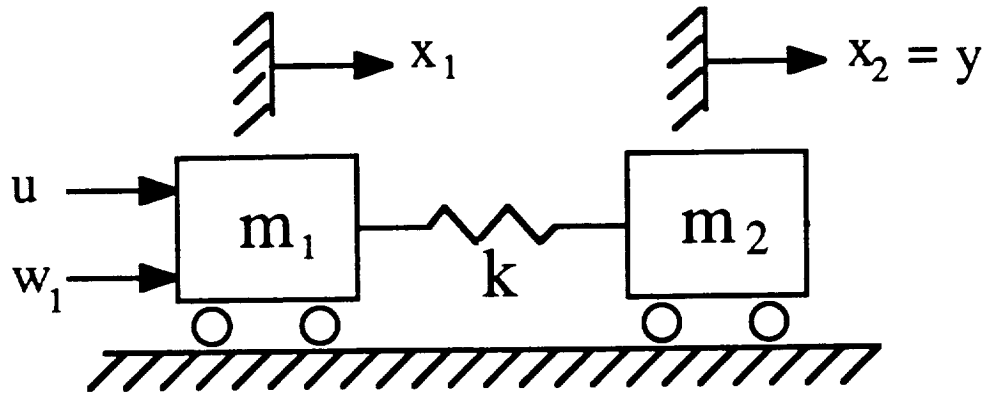

Figure 1: Two-mass-spring example.

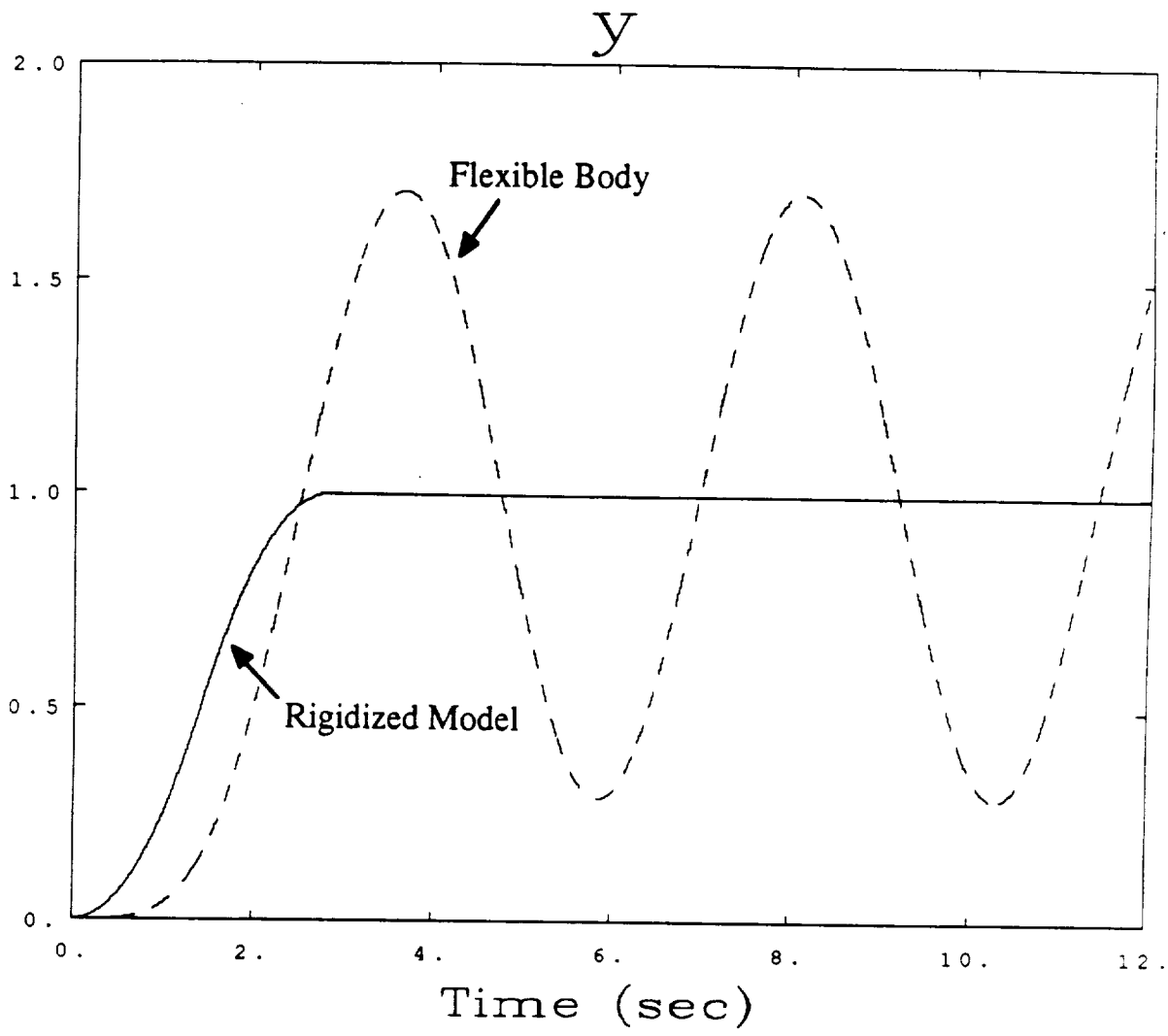

Figure 2: Responses to rigid-body, time-optimal control input.

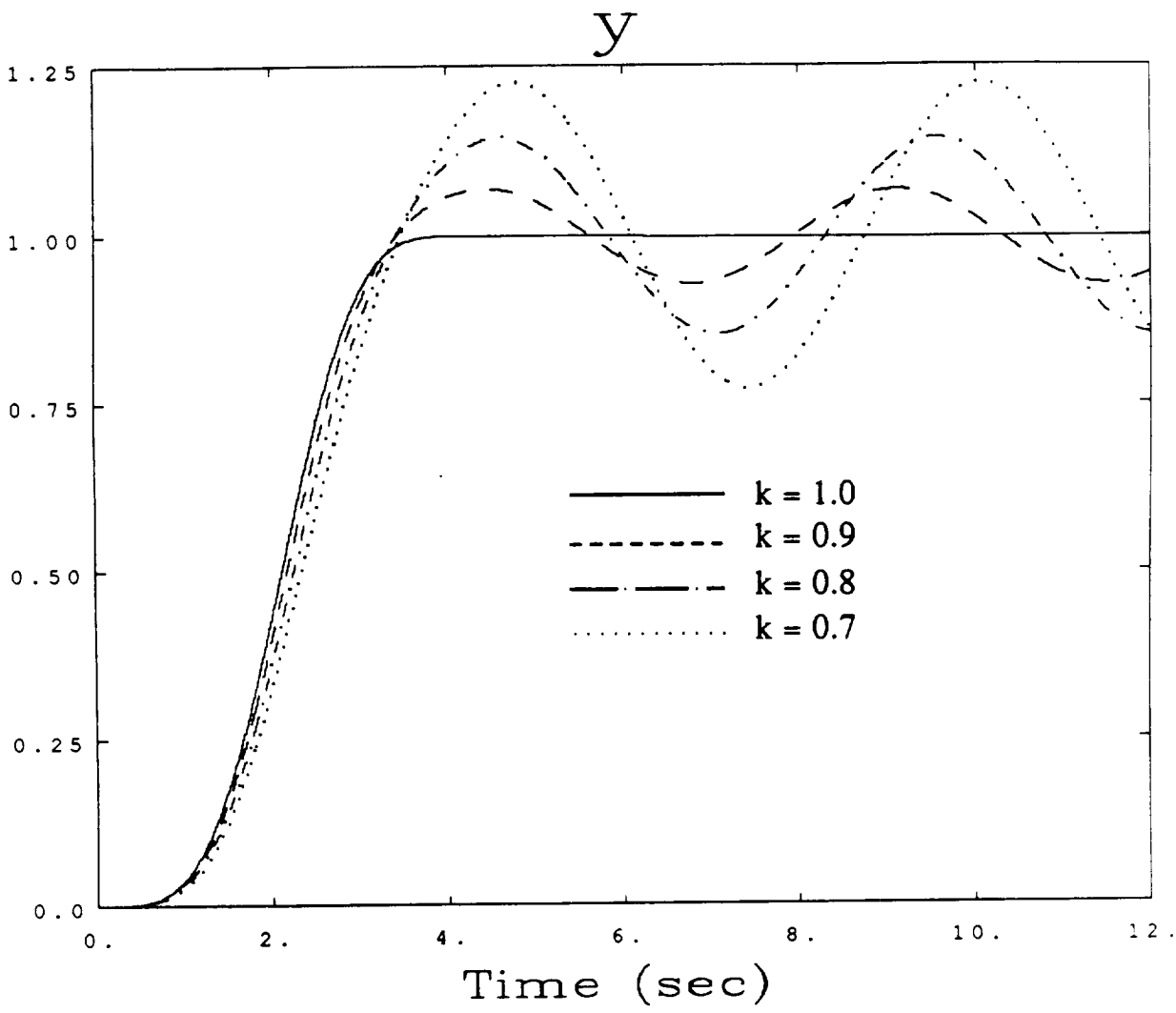

Figure 3: Responses to flexible-body, time-optimal control input.

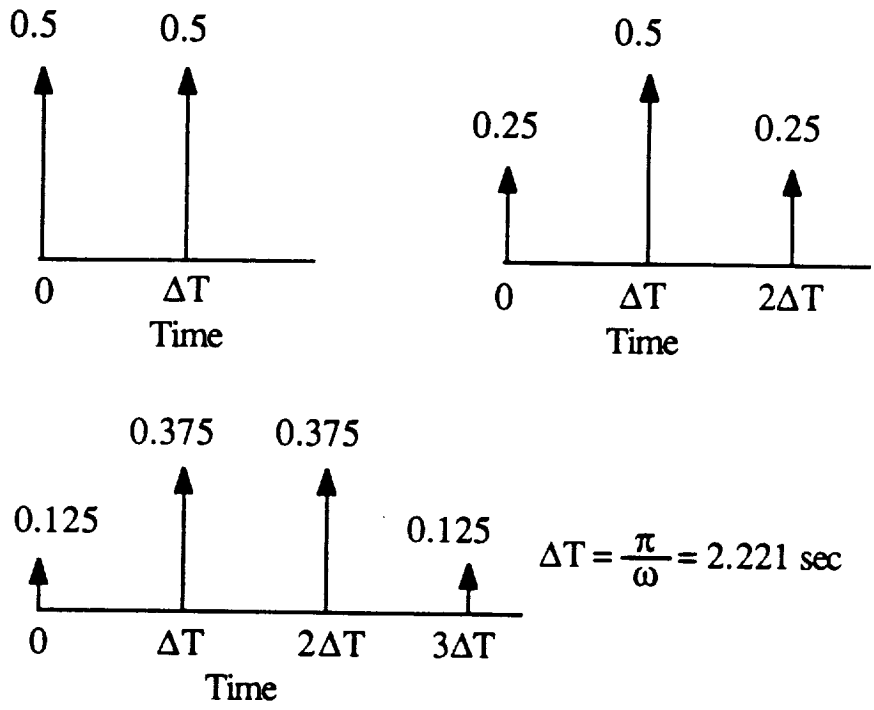

Figure 4: Impulse-sequence shaping.

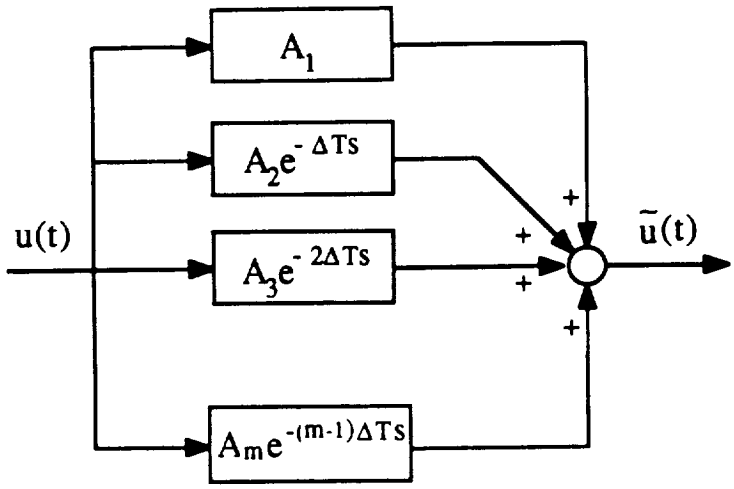

Figure 5: Tapped-delay filter.

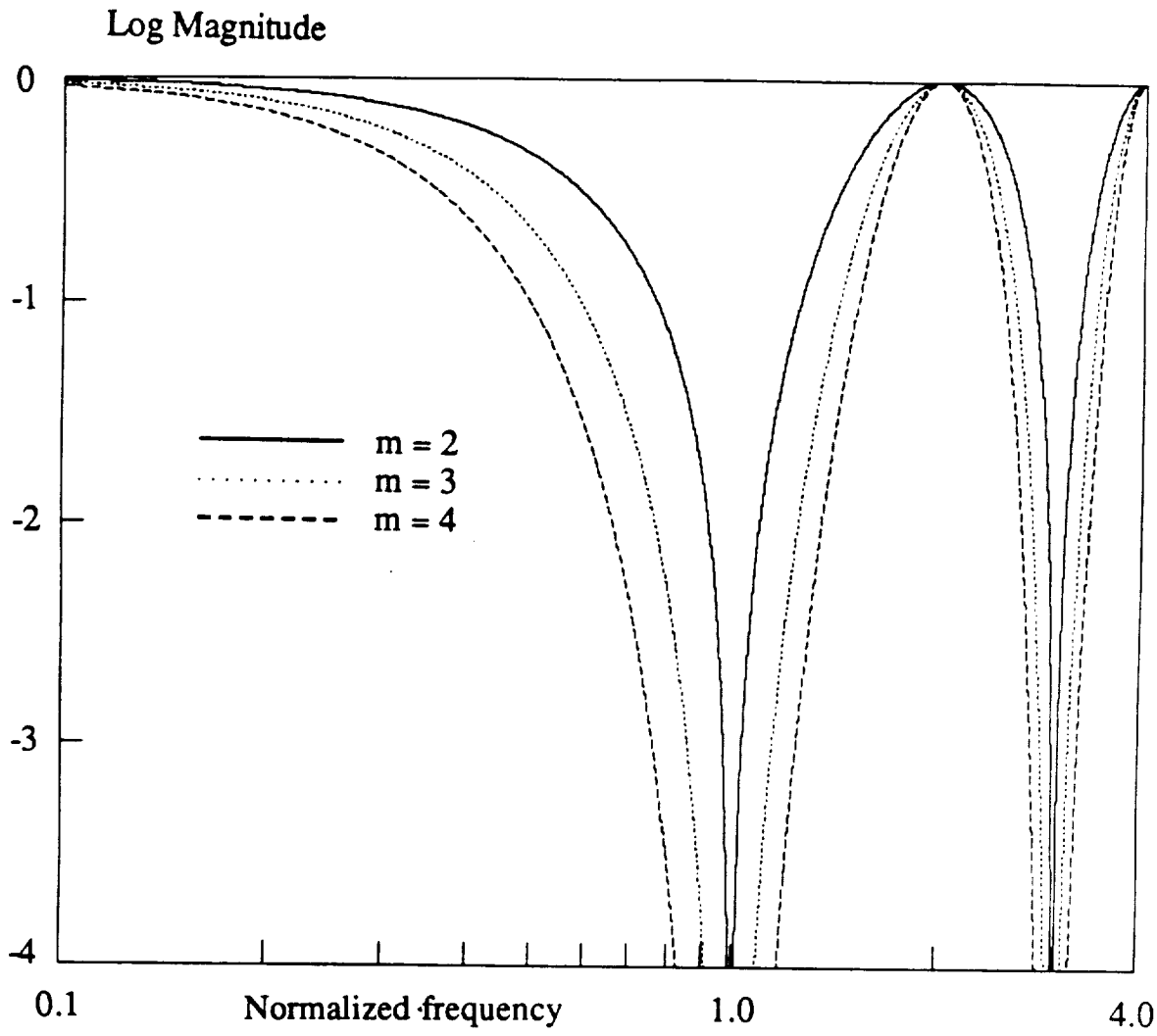

Figure 6: Frequency responses of tapped-delay filters with m =2, 3, 4.

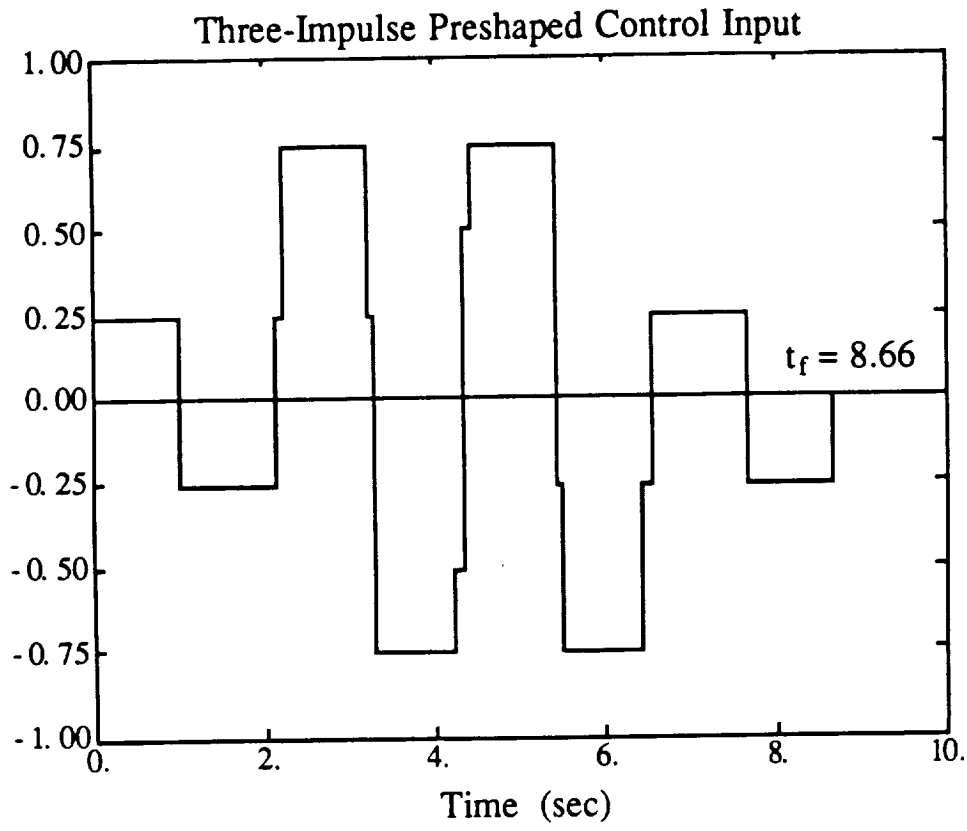

Figure 7: Flexible-body, time-optimal command, preshaped with tapped-delay filter with $m = 3$.

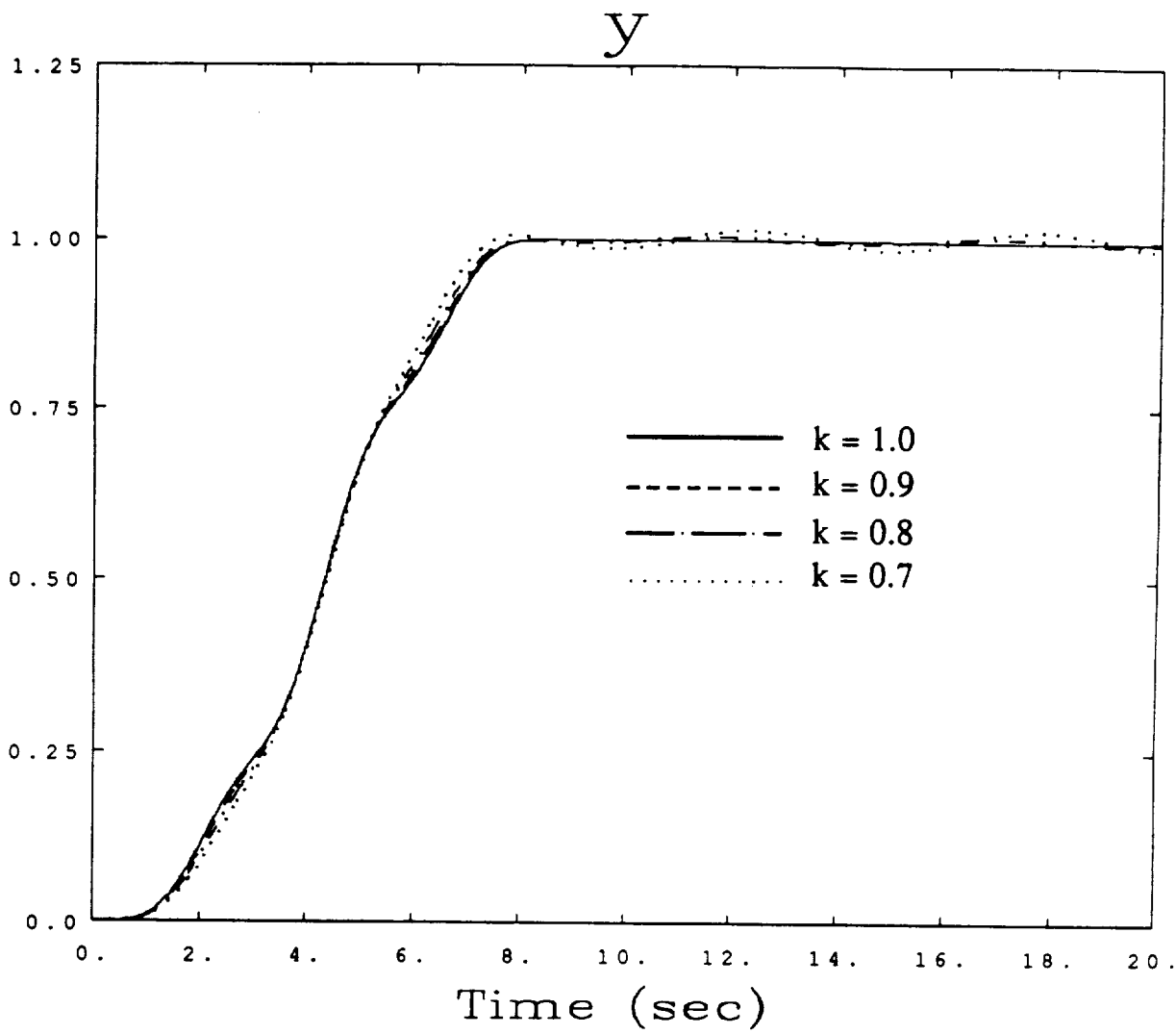

Figure 8: Responses to preshaped time-optimal command.

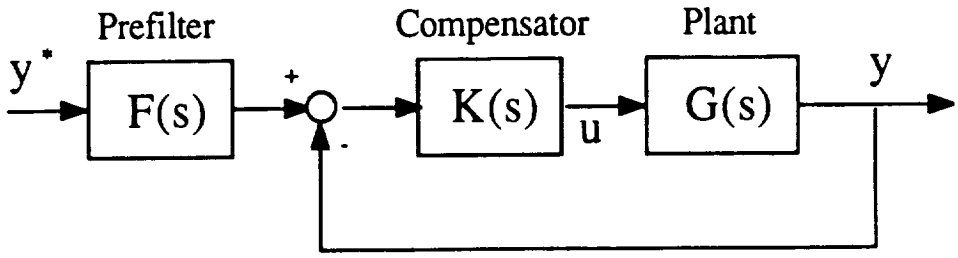

Figure 9: Conventional feedforward/feedback control system configuration.

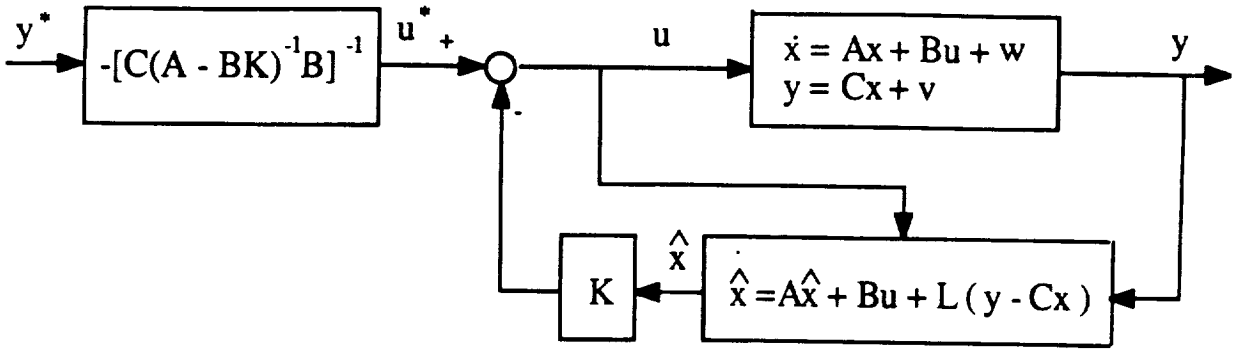

Figure 10: Control system configuration with LQG-type controller.

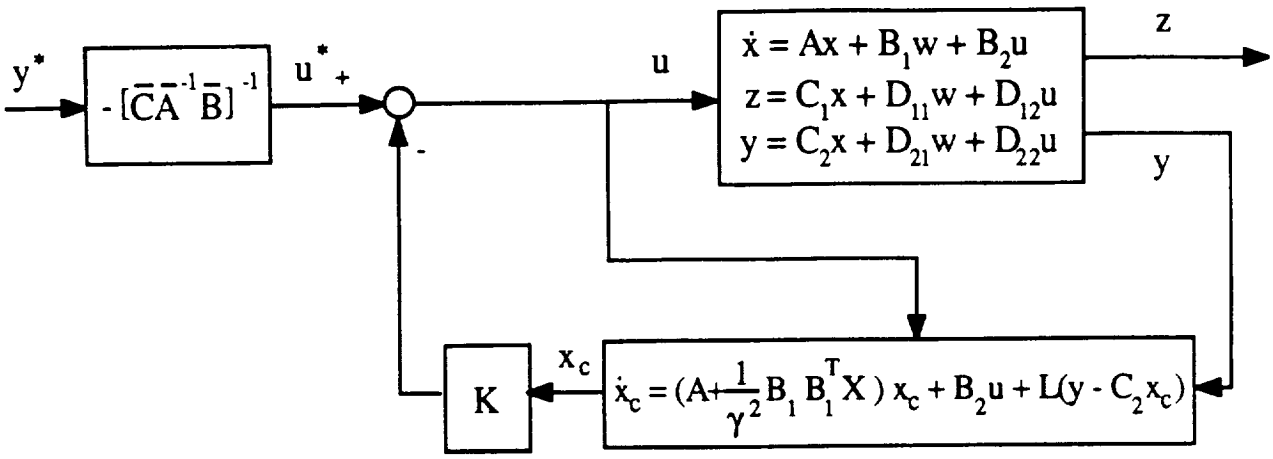

Figure 11: Control system configuration with H_∞-type controller.

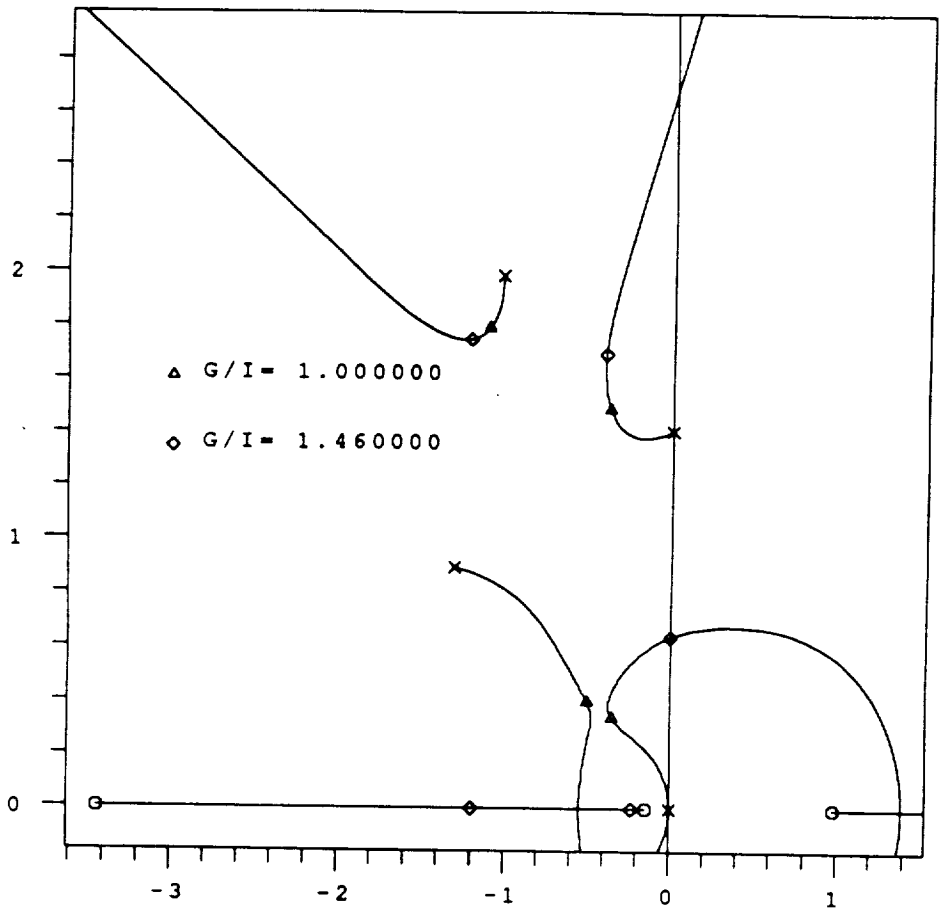

Figure 12: Root locus versus overall loop gain.

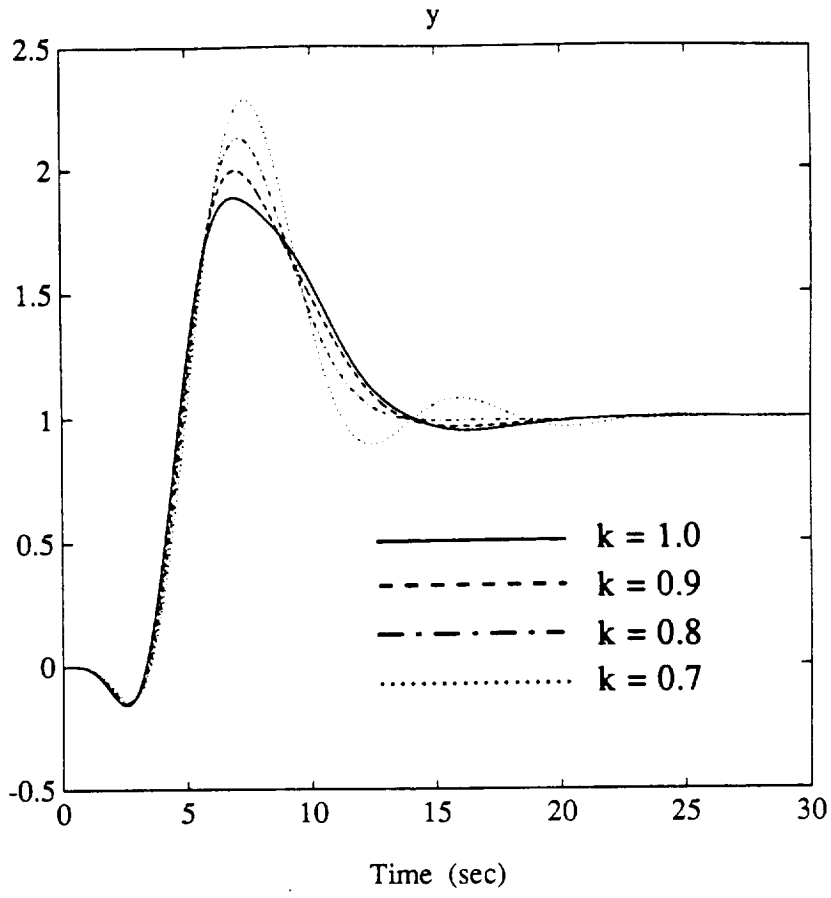

Figure 13: Time responses for conventional control configuration

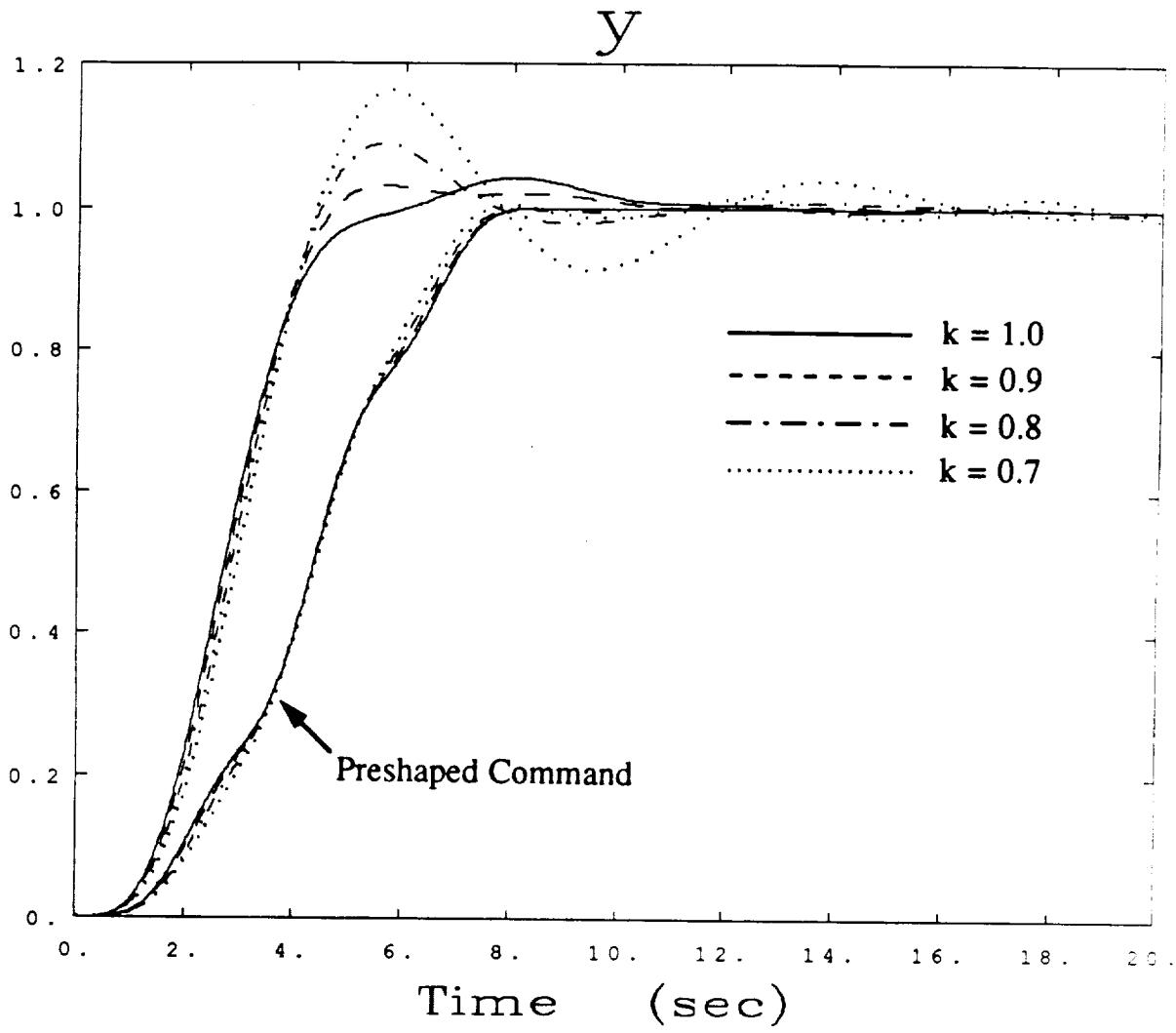

Figure 14: Time responses for non-zero set-point control configuration, compared with those shown in Fig. 8.

Robust Time-Optimal Control of Uncertain Flexible Spacecraft*

Qiang Liu† and Bong Wie‡
Arizona State University
Tempe, Arizona 85287

Abstract

A new approach for computing time-optimal open-loop control inputs for *uncertain* flexible spacecraft is developed. In particular, the single-axis, rest-to-rest maneuvering problem of flexible spacecraft in the presence of uncertainty in model parameters is investigated. Robust time-optimal control inputs are obtained by solving a parameter optimization problem subject to robustness constraints. A simple dynamical system with a rigid-body mode and one flexible mode is used to illustrate the concept.

1. Introduction

This paper is concerned with the problem of computing open-loop control inputs for flexible spacecraft, robotic manipulators and pointing systems in space, which are often required to maneuver as quickly as possible without significant structural vibrations during and/or after a maneuver.

A standard, time-optimal control approach to such a problem requires an accurate mathematical model, and thus the resulting solution is often sensitive to variations in model parameters. For this reason, an open-loop time-optimal controller is seldom used in practice. Consequently, the development of a "robustified" open-loop approach for a rapid maneuver without significant structural vibrations is of current research interest [1-3]. Other open-loop approaches [4-6] attempt to find a smooth continuous forcing function (e.g., a versine function) that begins and ends with zero slope. The basic idea

*AIAA Paper No. 91-2646, presented at the AIAA GN&C Conference, August 12-14, 1991, New Orleans, Louisiana.

†Graduate Research Assistant, Student Member AIAA.

‡Associate Professor, Dept. of Mechanical and Aerospace Engineering, Associate Fellow AIAA.

behind such approaches is that a smooth control input without sharp transitions is less likely to excite structural modes during maneuvers.

In this paper, a new approach is developed for computing time-optimal control inputs for the single-axis, rest-to-rest maneuvering problem of flexible spacecraft in the presence of structural mode frequency uncertainty. A parameter optimization problem, where the objective function to be minimized is the maneuvering time, is formulated with additional constraints for robustness with respect to structural parameter uncertainty. The resulting robust time-optimal solution is a multi-switch bang-bang control which can be implemented for spacecraft equipped with on-off reaction jets [7]. This result further confirms that most open-loop approaches, which utilize a smooth continuous control input so that structural modes are less likely to be excited, do not fully utilize the available control energy in performing a robust time-optimal maneuver.

The paper is organized as follows. In Section 2, the rest-to-rest maneuvering constraints for multi-switch bang-bang inputs are derived with some discussion on the previous results of [8-10] on the number of switchings for the time-optimal solution. The standard, time-optimal control problem is then transformed into a constrained parameter optimization problem. In Section 3, robustness constraints are derived and incorporated with the parameter optimization problem formulated in Section 2. A simple dynamical system with a rigid-body mode and one flexible mode, shown in Fig. 1, is used to illustrate the concept, and the robust time-optimal solution for a case with a single two-sided control (Case 1) is discussed. In Section 4, the same example with two one-sided control inputs (Case 2) is further investigated.

2. Time-Optimal Rest-to-Rest Maneuver

Problem Formulation

Consider a linear model of flexible spacecraft described by

$$M\ddot{x} + Kx = Gu \tag{1}$$

where x is a generalized displacement vector, M a mass matrix, K a stiffness matrix, G a control input distribution matrix and u a control input vector.

In this section, we consider a case with a scalar control input $u(t)$ bounded as

$$-1 \leq u \leq 1 \tag{2}$$

Equation (1) can be transformed into the decoupled modal equations:

$$\begin{aligned} \ddot{y}_1 + \omega_1^2 y_1 &= \phi_1 u \\ \ddot{y}_2 + \omega_2^2 y_2 &= \phi_2 u \\ &\vdots \\ \ddot{y}_n + \omega_n^2 y_n &= \phi_n u \end{aligned} \tag{3}$$

where y_i is the i^{th} modal coordinate, ω_i the i^{th} modal frequency, ϕ_i i^{th} modal gain, and n the number of modes considered in control design.

The problem is to find the control input which minimizes the performance index

$$J = \int_0^{t_f} dt = t_f$$

subject to Eqs. (2) and (3), and given boundary conditions.

The time-optimal control problem of a linear controllable system has a unique solution which is "bang-bang" control with a finite number of switches [10]. For a spring-mass dynamical system with n degrees of freedom, the time-optimal bang-bang solution for a rest-to-rest maneuver has, in most cases, $(2n-1)$ switches [8-9], and the solution is symmetric about $t_f/2$. That is, for a case with $(2n-1)$ switches, we have

$$t_j = t_{2n} - t_{2n-j}; \qquad j = 1, \cdots, n \tag{4}$$

where $t_{2n} = t_f$.

A bang-bang input with $(2n-1)$ switches can then be represented as:

$$u(t) = \sum_{j=0}^{2n} B_j u_s(t - t_j) \tag{5}$$

where B_j is the magnitude of a unit step function $u_s(t)$ at t_j. This function can be characterized by its switch pattern as:

$$\begin{aligned} B &= \{\ B_0,\quad B_1,\quad B_2,\ \cdots,\ B_{2n}\ \} \\ T &= \{\ t_0,\quad t_1,\quad t_2,\ \cdots,\ t_{2n}\ \} \end{aligned}$$

where B represents a set of B_j with $B_0 = B_{2n} = \pm 1$ and $B_j = \pm 2$ for $j = 1, \cdots, 2n-1$; T represents a set of switching times $(t_1, \cdots, t_{2n-1})$ and the initial and final times ($t_0 = 0$ and $t_f = t_{2n}$).

Rest-to-Rest Maneuver Constraints

Consider the rigid-body mode equation with $\omega_1 = 0$:

$$\ddot{y}_1 = \phi_1 u \tag{6}$$

with the rest-to-rest maneuvering boundary conditions

$$\begin{aligned} y_1(0) &= 0, \quad y_1(t_f) \neq 0 \\ \dot{y}_1(0) &= 0, \quad \dot{y}_1(t_f) = 0 \end{aligned} \tag{7}$$

Substituting Eq. (5) into Eq. (6) and solving for the time response of the rigid-body mode, we get

$$y_1(t \geq t_f) = \frac{\phi_1}{2} \sum_{j=0}^{2n} (t_f - t_j)^2 B_j \tag{8}$$

The rest-to-rest maneuvering constraint for the rigid-body mode can then be written as:

$$\frac{\phi_1}{2} \sum_{j=0}^{2n} (t_f - t_j)^2 B_j - y_1(t_f) = 0 \tag{9}$$

Consider now the structural modes described by

$$\ddot{y}_i + \omega_i^2 y_i = \phi_i u; \quad i = 2, \cdots, n \tag{10}$$

with the corresponding boundary conditions for the rest-to-rest maneuver:

$$\begin{aligned} y_i(0) &= 0, \quad y_i(t_f) = 0 \\ \dot{y}_i(0) &= 0, \quad \dot{y}_i(t_f) = 0 \end{aligned} \tag{11}$$

for each flexible mode.

Substituting Eq. (5) into the i^{th} structural mode equation and solving for the time response for $t \geq t_f$, we get

$$\begin{aligned} y_i(t) = & -\frac{\phi_i}{\omega_i^2} \sum_{j=0}^{2n} B_j \cos \omega_i (t - t_j) \\ = & -\frac{\phi_i}{\omega_i^2} [\cos \omega_i (t - t_n) \sum_{j=0}^{2n} B_j \cos \omega_i (t_j - t_n) \\ & + \sin \omega_i (t - t_n) \sum_{j=0}^{2n} B_j \sin \omega_i (t_j - t_n)] \end{aligned} \tag{12}$$

It can be shown that the following constraint equation for each mode

$$\sum_{j=0}^{2n} B_j \sin \omega_i (t_j - t_n) = 0 \tag{13}$$

is always satisfied for any bang-bang input which is symmetric about the mid-maneuver time t_n. Consequently, we have the following flexible mode constraints for no residual structural vibration (i.e., $y_i(t) = 0$ for $t \geq t_f$):

$$\sum_{j=0}^{2n} B_j \cos \omega_i (t_j - t_n) = 0 \tag{14}$$

for each flexible mode.

Parameter Optimization Problem

For a spring-mass system of n degrees of freedom, the time-optimal solution represented by Eq. (5) has the $(2n-1)$ unknown switching times and the final time t_f to be determined. The time-optimal control problem can now be formulated as a constrained parameter optimization problem as follows:

Determine a control of the form given by Eq. (5) that minimizes the final time t_f subject to

$$\frac{\phi_1}{2} \sum_{j=0}^{2n} (t_f - t_j)^2 B_j - y_1(t_f) = 0 \tag{15a}$$

$$\sum_{j=0}^{2n} B_j \cos \omega_i (t_j - t_n) = 0; \qquad i = 2, \cdots, n \tag{15b}$$

$$t_j > 0; \qquad j = 1, \cdots, 2n$$

where $t_f = t_{2n}$.

Remark: Note that ϕ_i $(i = 2, \cdots, n)$ do not appear in Eqs. (15); that is, the optimal solution to this problem is independent of the flexible mode shapes. In other words, the time-optimal control input is independent of actuator location for a system described by Eq. (3) with a scalar input.

Standard optimization packages (e.g., IMSL subroutines) can be used to obtain the solution of the above optimization problem. The major advantage of the proposed approach, compared to other direct numerical optimization approaches employed in [11-14] for the time-optimal control problem, is that some robustness constraints with respect to plant parameter uncertainty can be easily augmented. This subject will be discussed in detail in Section 3.

Sufficient Conditions for Optimality

Equations (15) are necessary conditions for time-optimal control, and sufficient conditions for optimality can be checked as follows.

Let the costate vector corresponding to the modal state vector $[y_1, \dot{y}_1, \omega y_2, \dot{y}_2, \cdots, \omega_n y_n, \dot{y}_n]^T$ be defined as

$$\lambda(t) = \left[\; p_1(t), \;\; q_1(t), \;\; \cdots, \;\; p_n(t), \;\; q_n(t) \; \right]^T \tag{16}$$

It is shown in [8] that at mid-maneuver, we have

$$\lambda(t_n) = \left[\; p_1(t_n), \;\; 0, \;\; p_2(t_n), \;\; 0, \;\; \cdots, \;\; p_n(t_n), \;\; 0 \; \right]^T \tag{17}$$

and thus the costate vector can be solved as

$$\begin{aligned} p_1(t) &= p_1(t_n) \\ q_1(t) &= -(t - t_n) p_1(t_n) \\ p_i(t) &= p_i(t_n) \cos \omega_i (t - t_n) \\ q_i(t) &= -p_i(t_n) \sin \omega_i (t - t_n) \end{aligned} \tag{18}$$

for each flexible mode. Then $p_i(t_n)$, for $i = 1, \cdots, n$, can be found from the following n linear equations:

$$1 + \phi_1 p_1(t_n) t_n + \sum_{i=2}^{n} \phi_i p_i(t_n) \sin \omega_i t_n = 0 \tag{19}$$

$$\phi_1 p_1(t_n)(t_j - t_n) + \sum_{i=2}^{n} \phi_i p_i(t_n) \sin \omega_i (t_j - t_n) = 0 \tag{20}$$

where $j = n+1, \cdots, 2n-1$.

The solution obtained by minimizing t_f subject to Eqs. (15) becomes time-optimal provided that

$$S(t) = -\phi_1 p_1(t_n)(t - t_n) - \sum_{i=2}^{n} \phi_i p_i(t_n) \sin \omega_i (t - t_n) \neq 0 \tag{21}$$

for $t \in (t_n, t_{2n})$ and $t \neq t_j$, $j = n+1, \cdots, 2n$, and $S(t)$ represents the switching function.

Remark: If modal frequencies are rational multiples of each other and the fundamental frequency, ω_2, satisfies the following relationship

$$\omega_2 = 2\ell\pi \sqrt{\frac{\phi_1}{y_1(t_f)}} \qquad \ell = 1, 2, \cdots \tag{22}$$

then the time-optimal solution has only one switch and is equivalent to the solution of a "rigidized" case.

Example: Case 1 with a Scalar Control Input

Consider a simple example, shown in Fig. 1, which is a generic representation of a flexible spacecraft with a rigid-body mode and one flexible mode. Case 1 with a scalar control input $u(t)$ is considered here. The equations of motion are

$$m_1\ddot{x}_1 + k(x_1 - x_2) = u_1 = u \tag{23a}$$

$$m_2\ddot{x}_2 - k(x_1 - x_2) = u_2 = 0 \tag{23b}$$

where x_1 and x_2 are the positions of body 1 and body 2, respectively, and the nominal parameters are $m_1 = m_2 = k = 1$ with appropriate units, and time is in units of second.

The boundary conditions for a rest-to-rest maneuver are given as

$$\begin{aligned} x_1(0) = x_2(0) = 0, \quad x_1(t_f) = x_2(t_f) = 1 \\ \dot{x}_1(0) = \dot{x}_2(0) = 0, \quad \dot{x}_1(t_f) = \dot{x}_2(t_f) = 0 \end{aligned} \tag{24}$$

The modal equations are

$$\ddot{y}_1 = u/2 \tag{25a}$$

$$\ddot{y}_2 + \omega^2 y_2 = u/2 \tag{25b}$$

where $\omega = \sqrt{2}$ rad/sec is the nominal flexible mode frequency. The corresponding boundary conditions for modal coordinates are

$$\begin{aligned} y_1(0) = y_2(0) = 0, \quad y_1(t_f) = 1, \; y_2(t_f) = 0 \\ \dot{y}_1(0) = \dot{y}_2(0) = 0, \quad \dot{y}_1(t_f) = \dot{y}_2(t_f) = 0 \end{aligned} \tag{26}$$

Since there are 3 switches, the time-optimal switch pattern for the given boundary conditions is represented as

$$\begin{aligned} B &= \{ \; B_0, \quad B_1, \quad B_2, \quad B_3, \quad B_4 \; \} \\ &= \{ \; 1, \quad -2, \quad 2, \quad -2, \quad 1 \; \} \\ T &= \{ \; t_0, \quad t_1, \quad t_2, \quad t_3, \quad t_4 \; \} \end{aligned}$$

with the symmetry conditions

$$t_4 = 2t_2$$

$$t_3 = 2t_2 - t_1$$

The time-optimal control problem is then formulated as the following constrained minimization problem:

$$min\ J = 2t_2 \tag{27}$$

subject to

$$2 + 2t_1^2 + t_2^2 - 4t_1 t_2 = 0$$
$$1 - 2\cos\omega(t_2 - t_1) + \cos\omega t_2 = 0$$
$$t_1,\ t_2 > 0;$$

A standard IMSL FORTRAN subroutine was used to obtain a solution as: $t_1 = 1.003$ and $t_2 = 2.109$. The computed solution satisfies the optimality conditions of Eq. (21); i.e., the switching function vanishes only at $t = t_1, t_2$ and t_3. Thus, the solution obtained via Eq. (27) is indeed time-optimal and it can be expressed as

$$u(t) = u_s(t) - 2u_s(t - 1.003) + 2u_s(t - 2.109) - 2u_s(t - 3.215) + u_s(t - 4.218) \tag{28}$$

The time responses of x_2 to the time-optimal control input are shown in Fig. 2 for four different values of k. It can be seen that the resulting responses are sensitive to variations in the model parameter k.

3. Robust Time-Optimal Control

As discussed in the preceding section, a standard, time-optimal control approach requires an accurate mathematical model and thus the resulting solution is often sensitive to plant modeling uncertainty.

In this section, a new approach, expanding on the approach introduced in Section 2, is developed for computing time-optimal control inputs for the single-axis, rest-to-rest maneuvering problem of flexible spacecraft in the presence of structural mode frequency uncertainty. A parameter optimization problem, where the objective function to be minimized is the maneuvering time, is formulated with additional constraints for robustness with respect to the structural frequency uncertainty. The resulting robustified, time-optimal soultion is a multi-switch bang-bang control, and is thus implementable for spacecraft equipped with on-off reaction jets [7].

Robustness Constraints

By taking the derivative of Eq. (12) with respect to ω_i, we get

$$\frac{dy_i(t)}{d\omega_i} = \frac{\phi_i}{\omega_i^2}\cos\omega_i(t-\frac{t_f}{2})\sum_{j=0}^{2n}(t_j-\frac{t_f}{2})B_j\sin\omega_i(t_j-\frac{t_f}{2}) \tag{29}$$

for each flexible mode. Letting $dy_i(t)/d\omega_i = 0$ for all $t \geq t_f$, we have

$$\sum_{j=0}^{2n}(t_j-\frac{t_f}{2})B_j\sin\omega_i(t_j-\frac{t_f}{2}) = 0; \qquad i = 2,\cdots,n \tag{30}$$

which is called the first-order robustness constraints.

Similarly, taking the derivative of Eq. (12) r_i times with respect to ω_i results in r_i^{th} order robustness constraints for each flexible mode as follows:

$$\sum_{j=0}^{2n}(t_j-\frac{t_f}{2})^m B_j\sin\omega_i(t_j-\frac{t_f}{2}) = 0$$
$$for\ m = 1,3,\cdots \leq r_i \tag{31a}$$
$$\sum_{j=0}^{2n}(t_j-\frac{t_f}{2})^m B_j\cos\omega_i(t_j-\frac{t_f}{2}) = 0$$
$$for\ m = 2,4,\cdots \leq r_i \tag{31b}$$

There are total r robustness constraints for $(n-1)$ flexible modes, where

$$r = \sum_{i=2}^{n} r_i \tag{32}$$

If these robustness constraints are included in the constrained minimization problem formulation described by Eq. (15), the number of switches in the bang-bang control input, in most cases, must be increased to match the number of the constraint equations. Due to the symmetric nature of the rest-to-rest maneuvering problem, adding one robustness constraint will require, at least, two more switches.

Robust Time-Optimal Control

If r robustness constraints are considered for a flexible spacecraft of n modes, the corresponding robustified bang-bang control input becomes

$$u(t) = \sum_{j=0}^{2(n+r)} B_j u_s(t-t_j) \tag{33}$$

which has $2(n+r)$ unknown switching times. Due to the symmetry property of the optimal solution for the rest-to-rest maneuvering problem, we have

$$t_j = t_{2(n+r)} - t_{2(n+r)-j}; \qquad j = 1, \cdots, n+r \tag{34}$$

Therefore, there are only $(n+r)$ unknowns to be determined in Eq. (33). These unknowns can be determined by minimizing t_f subject to the $(n+r)$ constraint equations: one positioning constraint for the rigid-body mode, $(n-1)$ no-vibration constraints and r robustness constraints.

While many theoretical issues (e.g., the uniqueness of the optimal solution) need to be explored, a solution can be obtained by solving the following constrained parameter optimization problem:

$$min\ J = t_f = t_{2(n+r)} \tag{35}$$

subject to

$$\frac{\phi_1}{2} \sum_{j=0}^{2(n+r)} (t_{2(n+r)} - t_j)^2 B_j - y_1(t_f) = 0$$

$$\sum_{j=0}^{2(n+r)} B_j \cos\omega_i(t_j - t_{n+r}) = 0$$

$$\sum_{j=0}^{2(n+r)} (t_j - t_{n+r})^m B_j \sin\omega_i(t_j - t_{n+r}) = 0;$$

$$for\ m = 1, 3, \cdots \leq r_i$$

$$\sum_{j=0}^{2(n+r)} (t_j - t_{n+r})^m B_j \cos\omega_i(t_j - t_{n+r}) = 0;$$

$$for\ m = 2, 4, \cdots \leq r_i$$

$$t_j > 0; \qquad j = 1, \cdots, 2(n+r)$$

for each flexible mode. The resulting bang-bang control input, which has $2r$ more switches than the time-optimal bang-bang solution of Section 2, is called a robust (or robustified) time-optimal solution in this paper.

Example: Case 1 with a Scalar Control Input

For Case 1, the time-optimal control is a three-switch bang-bang function, but the resulting responses were shown to be sensitive to variations in model parameter k . A robust time-optimal solution of the same problem is now developed as follows. The switching pattern for a case with the first-order robustness constraint is assumed as:

$$B = \{ B_0, \quad B_1, \quad B_2, \quad B_3, \quad B_4, \quad B_5, \quad B_6 \}$$
$$= \{ 1, \quad -2, \quad 2, \quad -2, \quad 2, \quad -2, \quad 1 \} \tag{36a}$$
$$T = \{ t_0, \quad t_1, \quad t_2, \quad t_3, \quad t_4, \quad t_5, \quad t_6 \} \tag{36b}$$

with the symmetry conditions

$$\begin{aligned} t_4 &= 2t_3 - t_2 \\ t_5 &= 2t_3 - t_1 \\ t_6 &= 2t_3 \end{aligned} \tag{37}$$

The constrained optimization problem with the first-order robustness constraint can be formulated as:

$$min\ J = t_6 \tag{38}$$

subject to

$$2 + 2t_1^2 - 2t_2^2 - t_3^2 - 4t_1t_3 + 4t_2t_3 = 0 \tag{39a}$$

$$\cos\omega t_3 - 2\cos\omega(t_3 - t_1) + 2\cos\omega(t_3 - t_2) - 1 = 0 \tag{39b}$$

$$t_3\sin\omega t_3 - 2(t_3 - t_1)\sin\omega(t_3 - t_1) + 2(t_3 - t_2)\sin\omega(t_3 - t_2) = 0 \tag{39c}$$

$$t_1,\ t_2,\ t_3 > 0;$$

A robust time-optimal solution with 5 switches can be found as:

$$\begin{aligned} t_1 &= 0.7124, \quad t_2 = 1.6563 \\ t_3 &= 2.9330, \quad t_4 = 4.2097 \\ t_5 &= 5.1536, \quad t_6 = 5.8660 \end{aligned} \tag{40}$$

The time responses of x_2 to this "robustified" time-optimal control input are shown in Fig. 3 for four different values of k. It can be seen that the resulting responses are less sensitive to parameter variations, compared to the responses to the ideal, time-optimal control input as shown in Fig. 2. Performance robustness has been increased at the expense of the increased maneuvering time of 5.866 sec, comparing to the ideal minimum-time of 4.218 sec. It is, however, emphasized that simply prolonging the maneuver time does not help to reduce residual structural vibrations caused by modeling uncertainty.

Remarks

An impulse-sequence shaping technique, developed by Singer and Seering [1,2], was employed by Wie and Liu [3] to preshape the ideal, time-optimal control input given in Eq. (28). For example, the two-impulse preshaped bang-bang command was obtained as

$$\begin{aligned} u(t) = {} & 0.5u_s(t) - u_s(t-1.003) + u_s(t-2.109) \\ & + 0.5u_s(t-2.221) - u_s(t-3.215) \\ & - u_s(t-3.224) + 0.5u_s(t-4.218) \\ & + u_s(t-4.330) - u_s(t-5.436) \\ & + 0.5u_s(t-6.439). \end{aligned} \tag{41}$$

This preshaped input takes values of ± 1.0 and ± 0.5, and the resulting response becomes less sensitive to flexible mode frequency variations as demonstrated in [3].

For Case 1, the time responses to the time-optimal input of Eq. (28), the robust time-optimal input of Fig. 3, and the preshaped inputs in [3] can be compared as shown in Figs. 4 and 5. Comparisons of the maneuvering times of four different control schemes are illustrated in Fig. 4. Parameter robustness with respect to spring constant variations is compared in Fig. 5 . From these figures, it is evident that the proposed approach of this paper provides a faster and more robust maneuver than other robustified feedforward approaches. Also, unlike other approaches in [1-6], the resulting solution of our new approach is a multi-switch bang-bang control which can be implemented for spacecraft with on-off reaction jets.

In the next section, we will consider a case with two one-sided control inputs in order to further explore a "time-optimal" actuator placement problem.

4. A Case with Two One-Sided Control Inputs

Problem Formulation

Consider Case 2, illustrated in Fig. 1, with two one-sided control inputs bounded as

$$0 \le u_1 \le +1 \tag{42a}$$

$$-1 \le u_2 \le 0 \tag{42b}$$

Since the control inputs are one-sided, each control input for the time-optimal solution need not be an odd function about the mid-maneuver time. Thus, the problem with one-sided control inputs becomes more difficult to solve than the standard problem with two-sided control inputs, and many theoretical issues (e.g., the uniqueness and structure of time-optimal solutions) need further investigation.

For Case 2, the modal equations of the system with nominal parameter values are

$$\ddot{y}_1 = \frac{1}{2}(u_1 + u_2) \tag{43a}$$

$$\ddot{y}_2 + \omega^2 y_2 = \frac{1}{2}(u_1 - u_2) \tag{43b}$$

where $\omega = \sqrt{2}$ rad/sec is the nominal flexible mode frequency.

For the control input constraint given by Eq. (42), the control inputs can be expressed as

$$u_1 = \sum_{j=0,2,4,\cdots}^{N-1} [u_s(t - t_j) - u_s(t - t_j - \Delta_j)] \tag{44a}$$

$$u_2 = -\sum_{j=1,3,5,\cdots}^{N} [u_s(t - t_j) - u_s(t - t_j - \Delta_j)] \tag{44b}$$

which is in the form of one-sided pulse sequences as shown in Fig. 6. The j^{th} pulse starts at t_j and ends at $(t_j + \Delta_j)$. Due to the symmetric nature of the rest-to-rest maneuvering problem, we assume that u_1 and u_2 have the same number of pulses, $(N + 1)/2$, where N is defined as in Fig. 6.

Substituting Eq. (44) into Eq. (43a) and solving for the time response of the rigid-body mode, we get

$$y_1(t \geq t_f) = \frac{1}{4}\sum_{j=0}^{N}(-1)^j[2t\Delta_j - 2t_j\Delta_j - \Delta_j^2] \tag{45}$$

For the desired boundary condition, $y_1(t \geq t_f) = 1$, the following constraint must hold

$$\sum_{j=0}^{N}(-1)^j\Delta_j = 0 \tag{46}$$

The positioning constraint for the rigid-body mode then becomes

$$\sum_{j=0}^{N}(-1)^j[2t_j\Delta_j + \Delta_j^2] + 4 = 0 \tag{47}$$

Substituting Eq. (44) into Eq. (43b) and solving for the time response of the flexible mode, we get

$$y_2(t) = -\frac{1}{4}\cos\omega t \sum_{j=0}^{N}[\cos\omega t_j - \cos\omega(t_j + \Delta_j)]$$
$$-\frac{1}{4}\sin\omega t \sum_{j=0}^{N}[\sin\omega t_j - \sin\omega(t_j + \Delta_j)] \tag{48}$$

for $t \geq t_f$.

Also, rest-to-rest maneuvering requires $y_2(t) = 0$ for $t \geq t_f$; i.e., we have

$$\sum_{j=0}^{N}[\cos\omega t_j - \cos\omega(t_j + \Delta_j)] = 0 \tag{49a}$$

$$\sum_{j=0}^{N}[\sin\omega t_j - \sin\omega(t_j + \Delta_j)] = 0 \tag{49b}$$

which become the no-vibration constraints for the rest-to-rest maneuvering problem.

Time-Optimal Control

Let the time-optimal control inputs for the rest-to-rest maneuver problem be of the form

$$u_1 = u_s(t) - u_s(t - \Delta)$$
$$u_2 = -u_s(t - t_1) + u_s(t - t_1 - \Delta)$$

where each input has a single pulse with the same pulse width of Δ, t_1 is defined as shown in Fig. 6, and the maneuver time $t_f = t_1 + \Delta$.

The rest-to-rest maneuver constraints can be obtained from Eqs. (47) and (49) as:

$$t_f - (2/\Delta) - \Delta = 0 \tag{50a}$$

$$\sin(\omega t_f/2) + \sin(\omega(\Delta - t_f/2)) = 0 \tag{50b}$$

which can be combined as:

$$\sin(\omega\Delta/2)\cos(\omega/(2\Delta)) = 0 \tag{51}$$

The time-optimal solution can then be obtained by solving the constrained minimization problem:

$$min\ J = t_f = (2/\Delta) + \Delta \tag{52}$$

subject to the constraint given by Eq. (51).

The solution of this problem can be found as

$$\Delta = 0.9003$$

$$t_f = 3.1218$$

The time responses of x_2 to the time-optimal control inputs are shown in Fig. 7 for four different values of k. The maneuver time and control on-time are respectively 3.12 sec and 1.8 sec. As expected, the resulting responses are sensitive to parameter variations.

Remark: A most interesting feature of this solution is that the overall input shape shown in Fig. 7 is of a "bang-off-bang" type, resulting in the control on-time of 1.8 sec which is different from the maneuver time t_f of 3.12 sec. For Case 1 and a rigidized case [3], both the maneuver time and control on-time are 4.218 sec and 2.828 sec, respectively. Therefore, the actuator configuration for Case 2 is considered to be "optimal" in the sense of minimizing both the maneuver time and control on-time.

Robust Time-Optimal Control

Similar to Case 1 in Section 2, we now consider the "robustification" of the time-optimal solution obtained in the preceding section.

Letting the derivative of Eq. (48) with respect to ω be zero, we get

$$\begin{aligned}\frac{dy_2}{d\omega} = & -\frac{1}{4}\sin\omega t \sum_{j=0}^{N}[t_j \cos\omega t_j - (t_j+\Delta_j)\cos\omega(t_j+\Delta_j)] \\ & + \frac{1}{4}\cos\omega t \sum_{j=0}^{N}[t_j \sin\omega t_j - (t_j+\Delta_j)\sin\omega(t_j+\Delta_j)] \\ = & \ 0 \end{aligned} \tag{53}$$

For this derivative to be zero for arbitary $t \geq t_f$, we must have

$$\sum_{j=0}^{N}[t_j \cos\omega t_j - (t_j+\Delta_j)\cos\omega(t_j+\Delta_j)] = 0 \tag{54a}$$

$$\sum_{j=0}^{N}[t_j \sin\omega t_j - (t_j+\Delta_j)\sin\omega(t_j+\Delta_j)] = 0 \tag{54b}$$

which is called the first-order robustness constraints.

Taking the derivative of Eq. (48) r times with respect to ω, we get the r^{th}-order robustness constraint equations for input pulse sequences as follows:

$$\sum_{j=0}^{N}[(t_j)^m \cos\omega t_j - (t_j+\Delta_j)^m \cos\omega(t_j+\Delta_j)] = 0 \tag{55}$$

$$\sum_{j=0}^{N}[(t_j)^m \sin\omega t_j - (t_j+\Delta_j)^m \sin\omega(t_j+\Delta_j)] = 0 \tag{56}$$

for $m = 1, 2, \cdots, r$.

As an example, we consider the first-order robustness constraint, incorporated with the rest-to-rest maneuver constraints, to construct robust time-optimal pulse sequences. Assuming that each input has two pulses, we can represent the control inputs as follows:

$$\begin{aligned} u_1 = {} & u_s(t) - u_s(t-\Delta_0) + u_s(t-t_2) \\ & - u_s(t-t_2-\Delta_2) \end{aligned} \tag{57a}$$

$$\begin{aligned} u_2 = {} & -u_s(t-t_1) + u_s(t-t_1-\Delta_1) - u_s(t-t_3) \\ & + u_s(t-t_3-\Delta_3) \end{aligned} \tag{57b}$$

in which we have seven unknowns to be determined, and t_j and Δ_j are defined as shown in Fig. 6.

The robust time-optimal solution can then be obtained by solving the constrained parameter optimization problem

$$min\ J = t_3 + \Delta_3 \tag{58}$$

subject to

$$\Delta_0 - \Delta_1 + \Delta_2 - \Delta_3 + \Delta_4 = 0$$

$$\sum_{j=0}^{3}(-1)^j[2t_j\Delta_j + \Delta_j^2] + 4 = 0$$

$$\sum_{j=0}^{3}[\cos\omega t_j - \cos\omega(t_j+\Delta_j)] = 0$$

$$\sum_{j=0}^{3}[\sin\omega t_j - \sin\omega(t_j+\Delta_j)] = 0$$

$$\sum_{j=0}^{3}[t_j\cos\omega t_j - (t_j+\Delta_j)\cos\omega(t_j+\Delta_j)] = 0$$

$$\sum_{j=0}^{3}[t_j \sin\omega t_j - (t_j + \Delta_j)\sin\omega(t_j + \Delta_j)] = 0$$

$$\Delta_j \geq 0; \quad j = 0, 1, 2, 3$$

$$t_1,\ t_2,\ t_3 > 0$$

The solution to this problem can be obtained as:

$$\begin{aligned} t_0 &= 0.0000, \quad \Delta_0 = 0.4274 \\ t_1 &= 2.3357, \quad \Delta_1 = 0.4329 \\ t_2 &= 2.1132, \quad \Delta_2 = 0.4329 \\ t_3 &= 4.4544, \quad \Delta_3 = 0.4274 \end{aligned} \tag{60}$$

The time responses of x_2 to the robust time-optimal control inputs are shown in Fig. 8 for four different values of k. It is seen that the robustness has been increased at the expense of the increased maneuvering time of 4.882 sec, comparing with the ideal minimum-time of 3.122 sec. However, note that the control on-time is only 1.721 sec, compared to the control on-time of 1.8 sec of the ideal, time-optimal solution.

6. Conclusions

A new approach to the *robust* time-optimal control of *uncertain* flexible spacecraft has been investigated. The unique feature of the proposed approach is the fairly straightforward incorporation of the robustness constraints into a standard parameter optimization problem, where the objective function to be minimized is the maneuvering time. The case with two one-sided control inputs has shown an interesting feature from the viewpoint of "optimal" actuator placement for minimizing both the maneuver time and control on-time.

Acknowledgments

This research was supported by the NASA Johnson Space Center through the RICIS program of the University of Houston at Clear Lake. The authors would like to express special thanks to Dr. Kenneth Cox and Dr. John Sunkel at NASA JSC for their sponsoring this research for possible applications to real space vehicles. The authors would also like to thank Prof. Karl Bilimoria for his thorough review of this paper and for his technical assistance.

References

[1] N.C. Singer and W.P. Seering, "Using Acausal Shaping Techniques to Reduce Robot Vibration," *Proc. of the 1988 IEEE International Conference on Robotics and Automation*, Philadelphia, PA, April 25-29, 1988.

[2] N.C. Singer and W.P. Seering, "Preshaping Command Inputs to Reduce System Vibration," *Proc. of the 1989 IEEE International Conference on Robotics and Automation*, Scottsdale, Arizona, May, 1989.

[3] B. Wie and Q. Liu, "A Comparison Between Robustified Feedforward and Feedback for Achieving Performance Robustness," AIAA Paper No. 90-3424, to appear in the *Journal of Guidance, Control and Dynamics.*

[4] C.J. Swigert, "Shaped Torque Techniques," *Journal of Guidance and Control*, Vol. 3, No. 5, Sept.-Oct., 1980, pp. 460–467.

[5] D.M. Aspinwall, "Acceleration Profiles for Minimizing Residual Response," *Journal of Dynamic Systems, Measurement and Control*, Vol.102, March 1980, pp. 3–7.

[6] R.M. Byers, S.R. Vadali and J.L. Junkins, "Near-Minimum Time, Closed-Loop Slewing of Flexible Spacecraft," *Journal of Guidance, Control and Dynamics*, Vol. 13, No. 1, 1990, pp. 57–65.

[7] T.C. Anthony, B. Wie and S. Carroll, "Pulse Modulated Control Synthesis for a Flexible Spacecraft," *Journal of Guidance, Control and Dynamics*, Vol. 13, No. 6, 1990, pp.1014–1022.

[8] G. Singh, P.T. Kabamba, and N.H. McClamroch, "Planar, Time-Optimal, Rest-to-Rest Slewing Maneuvers of Flexible Spacecraft," *Journal of Guidance, Control and Dynamics*, Vol. 12, No. 1, 1989, pp. 71–81.

[9] L.Y. Pao and G.F. Frankin, "Time-Optimal Control of Flexible Structures," *Proc. of the 29th IEEE Conference on Decision and Control*, Honolulu, Hawaii, December 1990, pp. 2580–2581.

[10] H. Hermes and J. LaSalle, *Functional Analysis and Time Optimal Control,* Academic Press, New York, 1969.

[11] E.B. Meier and A.E. Bryson,"Efficient Algorithm for Time-Optimal Control of a Two-Link Manipulator," *Journal of Guidance, Control and Dynamics*, Vol. 13, No. 5, 1990, pp. 859-866.

[12] Y. Zhao, A.E. Bryson, and R. Slattery, "Generlaized Gradient Algorithm for Trajectory Optimization," *Journal of Guidance, Control and Dynamics*, Vol. 13, No. 6, 1990, pp.1166–1169.

[13] B. Wie, C.-H. Chuang and J. Sunkel, "Minimum-Time Pointing Control of a Two-Link Manipulator," *Journal of Guidance, Control and Dynamics*, Vol. 13, No. 5, 1990, pp. 867-873.

[14] K. Bilimoria and B. Wie, "Minimum-Time Three-Axis Reorientation of a Rigid Spacecraft," AIAA Paper No. 90-3486, to appear in the *Journal of Guidance, Control and Dynamics*

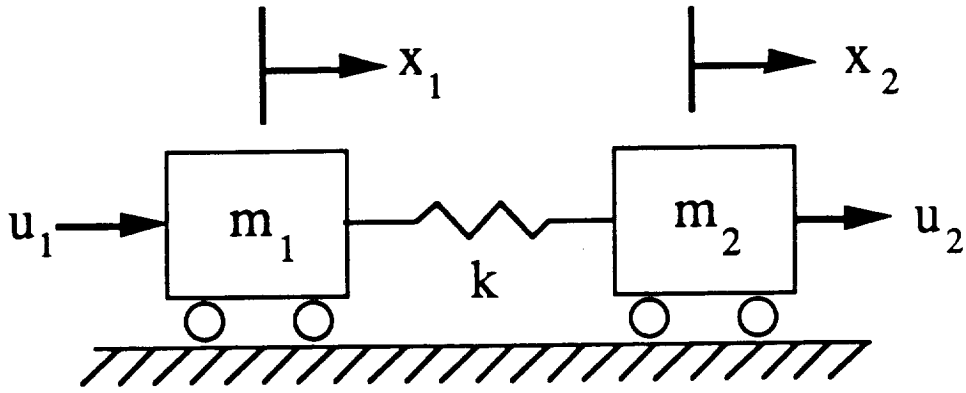

Case 1: $-1 \leq u_1 \leq 1$; $u_2 = 0$

Case 2: $0 \leq u_1 \leq 1$; $-1 \leq u_2 \leq 0$

Figure 1: Generic model with a rigid-body mode and one flexible mode.

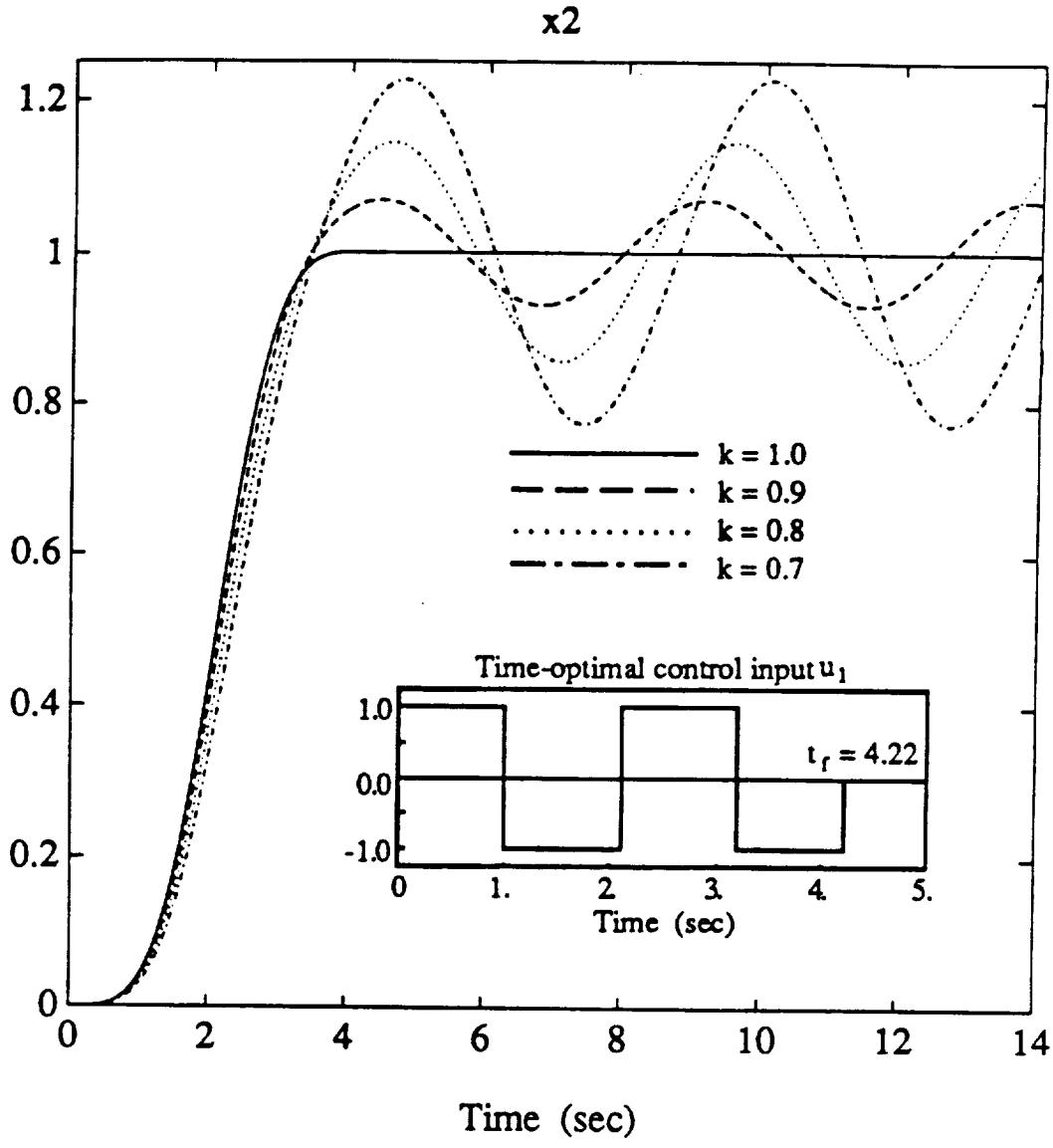

Figure 2: Responses to time-optimal control input (Case 1).

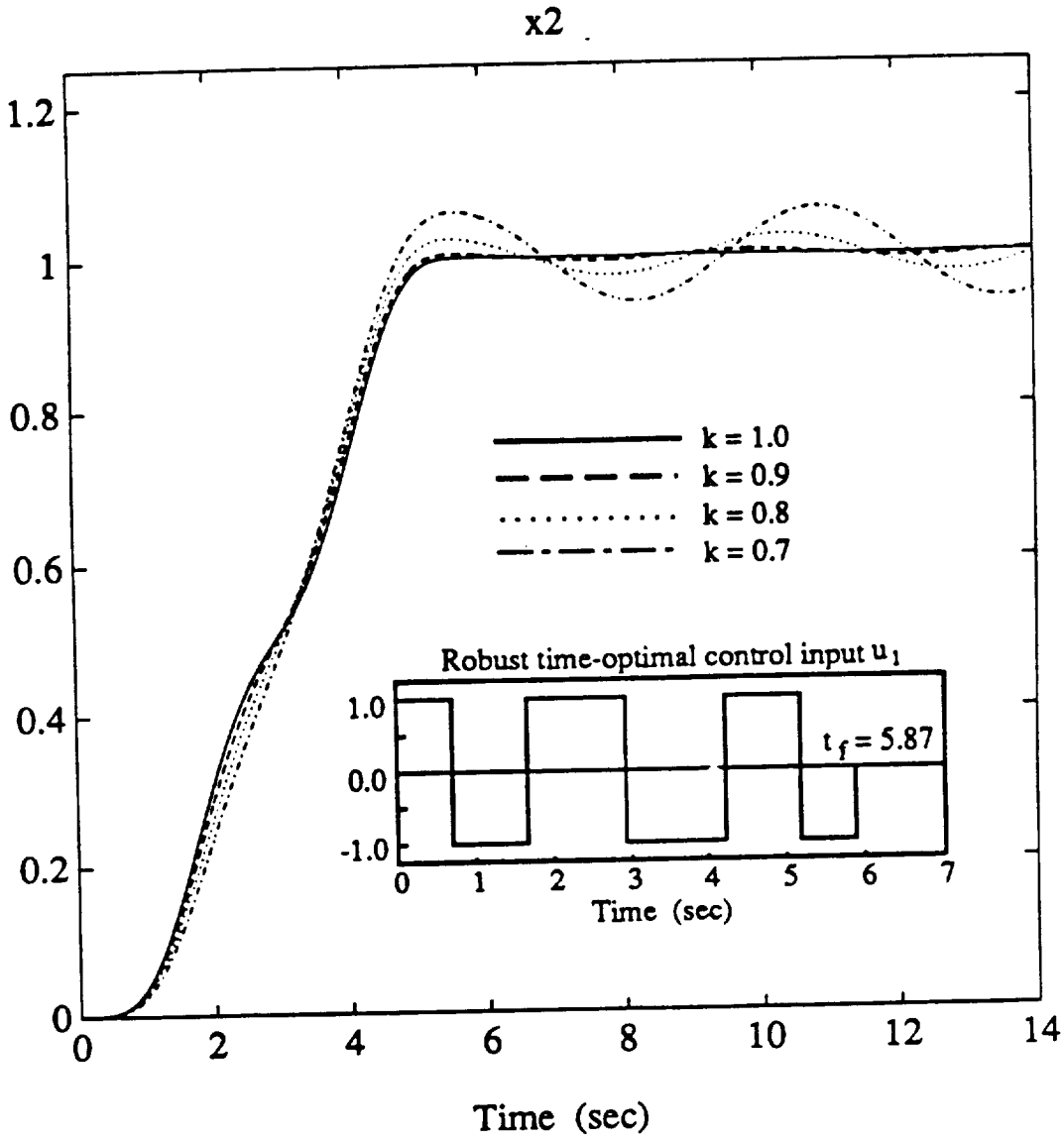

Figure 3: Responses to robust time-optimal control input (Case 1).

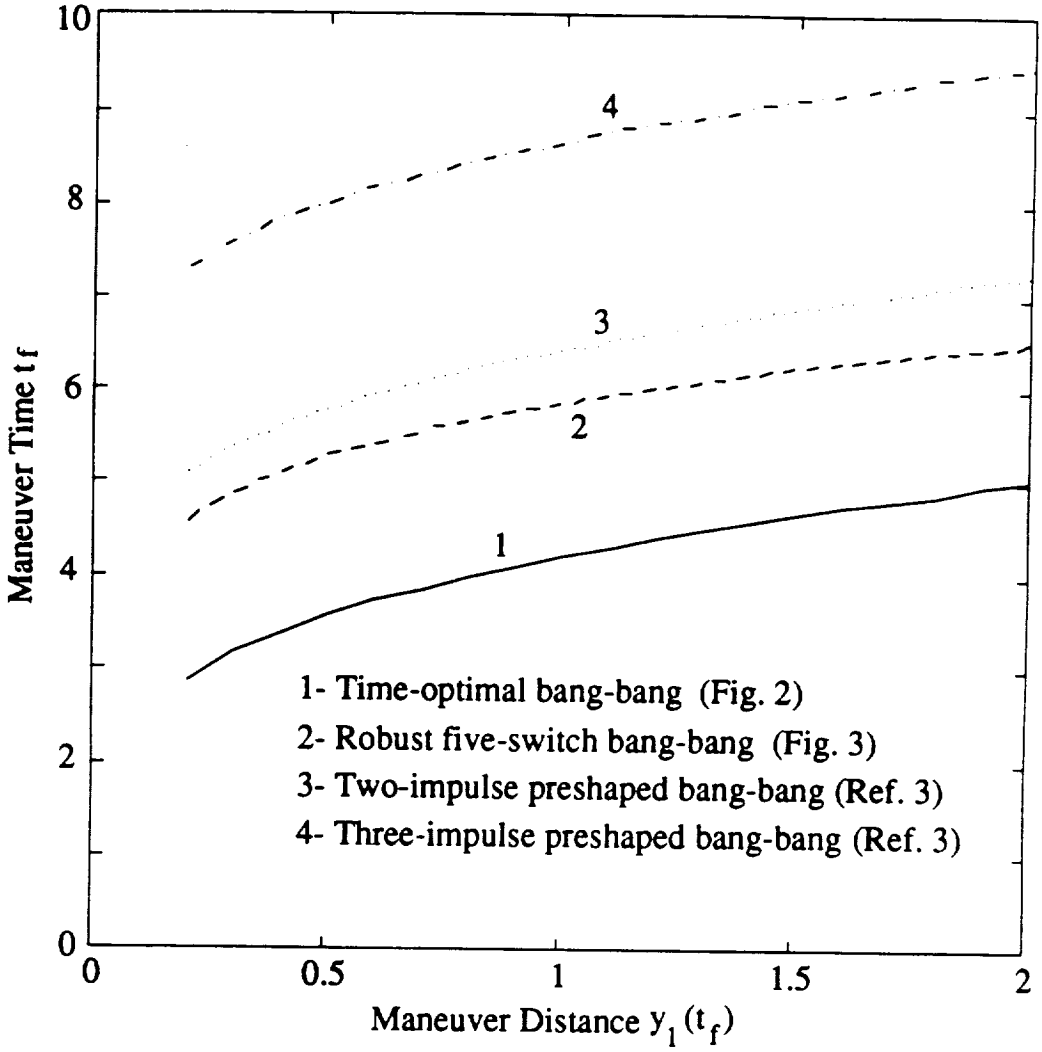

Figure 4: Comparision of maneuvering time.

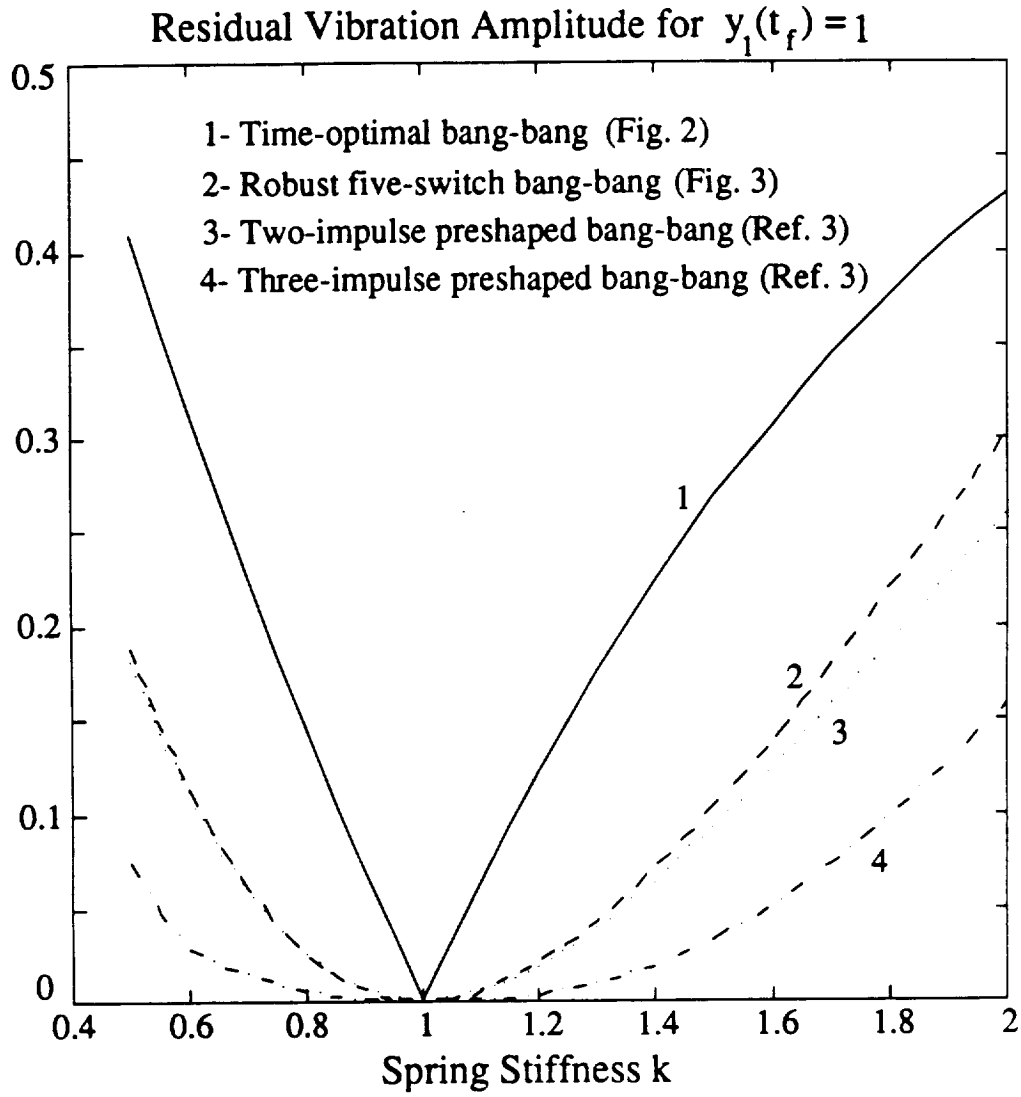

Figure 5: Comparision of parameter sensitivity

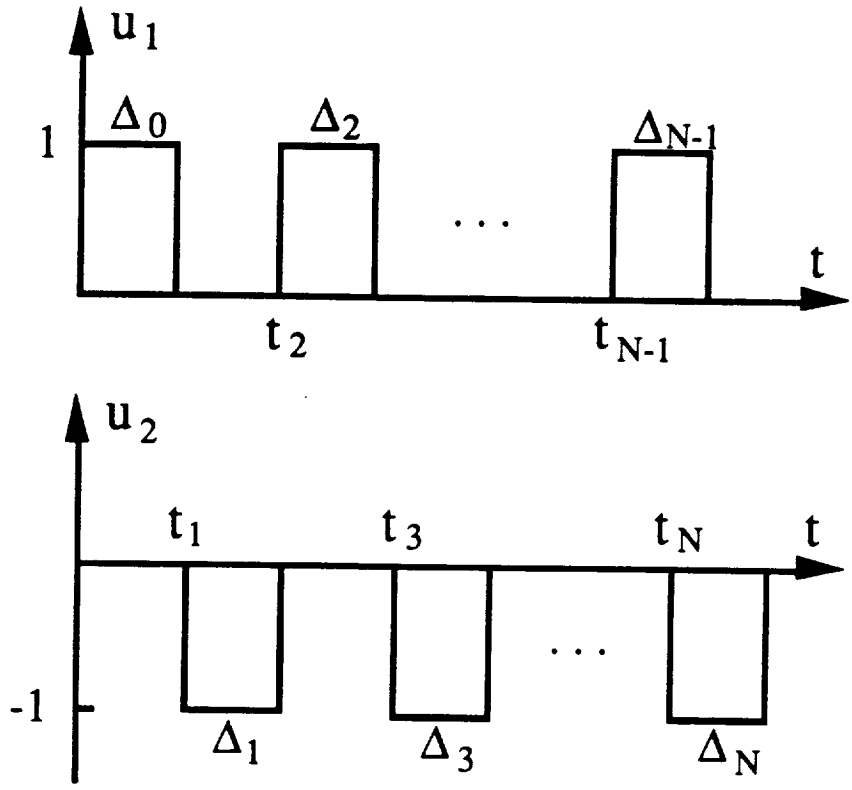

Figure 6: Pulse sequences (Case 2).

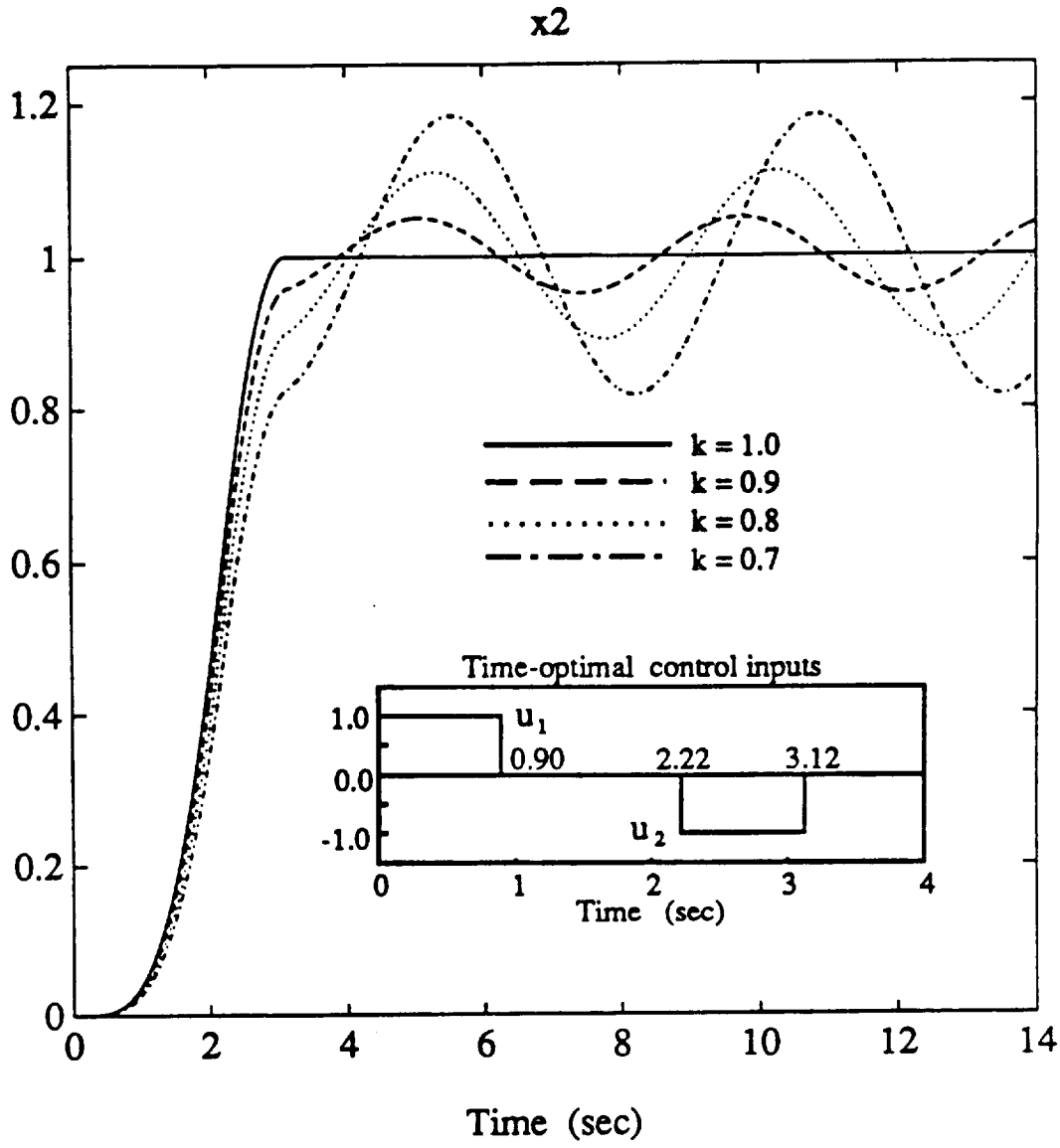

Figure 7: Responses to time-optimal control inputs (Case 2).

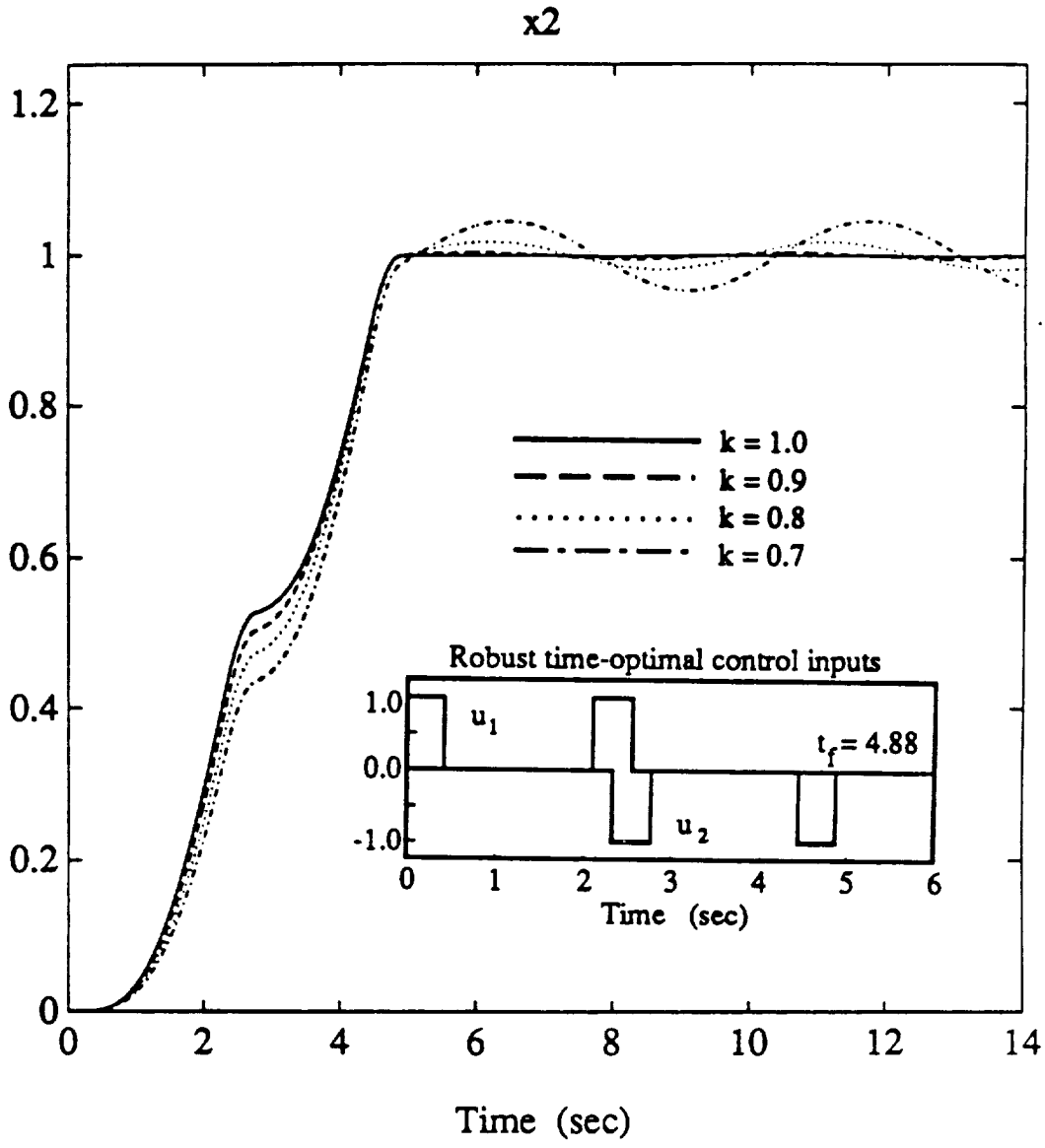

Figure 8: Responses to robust time-optimal control inputs (Case 2).

On Actuator Placement for Robust Time-Optimal Control of Flexible Spacecraft

Bong Wie,* Ravi Sinha,† and Qiang Liu†
Arizona State University
Tempe, AZ 85287-6106

Abstract

The problem of computing open-loop, on-off jet firing logic for flexible spacecraft in the face of plant modeling uncertainty is investigated. The primary control objective is to achieve a fast maneuvering time with a minimum of structural vibrations during and/or after a maneuver. This paper is also concerned with the problem of selecting a proper pair of jets for practical trade-offs among the maneuvering time, fuel consumption, structural mode excitation, and performance robustness. A time-optimal control problem subject to parameter robustness constraints is formulated. A three-mass-spring model of flexible spacecraft with a rigid-body mode and two flexible modes is used to illustrate the concept.

*Associate Professor, Dept. of Mechanical and Aerospace Engineering, Associate Fellow AIAA.
†Graduate Research Assistants, Student Member AIAA.

1. Introduction

This paper deals with the problem of computing open-loop, on-off jet firing logic for flexible spacecraft which are sometimes required to maneuver as quickly as possible with a minimum of structural vibrations during and/or after a maneuver. Most standard time-optimal control approaches to such a problem require an accurate mathematical model, and thus the resulting solution becomes sensitive to variations in model parameters.

Expanding on the recent results of [1-2], we further explore the robust time-optimal control problem of flexible spacecraft in the face of modeling uncertainty. In particular, we study the problem of selecting a proper pair of jets for practical trade-offs among the maneuvering time, fuel consumption, structural mode excitation, and performance robustness. A parameter optimization approach, with additional constraints for performance robustness with respect to modeling uncertainty, is employed to solve such a robust time-optimal control problem. However, many theoretical and practical implementation issues inherent to constrained parameter optimization problems are not elaborated in this paper.

A simple math model of flexible spacecraft with a rigid-body mode and two flexible modes, as shown in Fig. 1, is used to illustrate the concept and methodology. We consider the case in which the structural flexibility and mass distribution of the vehicle are quite uncertain, while the total mass (or inertia) of the vehicle is well known. Consequently, we focus on the robust control problem of flexible spacecraft in the face of modal frequency uncertainty as well as mode shape uncertainty.

Other robustified, open-loop approaches, however, attempt to find a smooth continuous forcing function (e.g., a versine function) that begins and ends with zero slope. The basic idea behind such approaches is that a smooth control input without sharp transitions is less likely to excite structural modes during maneuvers. On the contrary to such a common notion, the results of this paper indicate that properly modulated, on-off pulse sequences can achieve a fast maneuvering time with a minimum of structural vibrations during and/or after a maneuver, even in the face of plant modeling uncertainty.

The remainder of this paper is organized as follows. Section 2 describes the standard time-optimal control problem of flexible spacecraft without modeling uncertainty. A

parameter optimization problem is formulated, in which the objective function is the maneuvering time. Three cases are explored, as illustrated in Fig. 1, in order to assess the actuator placement problem for time-optimal control of flexible spacecraft with multiple jets. In Section 3, we investigate the same problem as in Section 2 but considering the presence of modeling uncertainty. A time-optimal control problem subject to additional robustness (or sensitivity) constraints is formulated, and numerical solutions for three cases are then compared with solutions obtained in Section 2.

2. Time-Optimal Rest-to-Rest Maneuver Control

Problem Formulation

Consider a flexible spacecraft described by

$$M\ddot{x} + Kx = Gu \tag{1}$$

where x is a generalized displacement vector, M a mass matrix, K a stiffness matrix, G the control input distribution matrix, and u the control input vector.

Equation (1) is transformed into the modal equations:

$$\begin{aligned} \ddot{y}_1 + \omega_1^2 y_1 &= \phi_{11}u_1 + \phi_{12}u_2 + \phi_{13}u_3 \\ \ddot{y}_2 + \omega_2^2 y_2 &= \phi_{21}u_1 + \phi_{22}u_2 + \phi_{23}u_3 \\ &\vdots \\ \ddot{y}_n + \omega_n^2 y_n &= \phi_{n1}u_1 + \phi_{n2}u_2 + \phi_{n3}u_3 \end{aligned} \tag{2}$$

where y_i is the i^{th} modal coordinate, ω_i the i^{th} modal frequency, ϕ_{ij} the modal input distribution coefficient, and n the number of modes considered in control design. Without loss of generality, only three control inputs are considered in Eq. (2).

In this paper, we consider a simple model which is a generic representation of a spacecraft with a rigid-body mode and two flexible modes, as shown in Fig. 1. Three cases are studied: (i) Case 1 with both "positive" and "negative" jets placed at body 1, (ii) Case 2 with a "positive" jet at body 1 and a "negative" jet at body 2, and (iii) Case 3 with a "positive" jet at body 1 and a "negative" jet at body 3. Case 1 is a typical case in which two opposing jets are colocated. In Cases 2 and 3, two opposing jets are not colocated.

For a class of problems, such as Case 1, the modal equations become

$$\ddot{y}_i + \omega_i^2 y_i = \phi_i u; \quad i = 1, \cdots, n \tag{3}$$

where ϕ_i the i^{th} modal gain and the scalar control input u is bounded as

$$-1 \leq u \leq 1 \tag{4}$$

The problem is to find the control input $u(t)$ which minimizes the performance index

$$J = \int_0^{t_f} dt = t_f$$

subject to Eqs. (3) and (4), and given boundary conditions. The time-optimal bang-bang solution of this problem with the rest-to-rest maneuvering boundary conditions has, in most cases, $(2n-1)$ switches, and the solution is symmetric about the mid-maneuver time $t_f/2$ [2]. That is, for a case with $(2n-1)$ switches, we have the symmetric switching pattern given as:

$$t_j = t_{2n} - t_{2n-j}; \qquad j = 1, \cdots, n \tag{5}$$

where t_j is the j^{th} switching time and $t_{2n} = t_f$.

A bang-bang input with $(2n-1)$ switches is expressed as

$$u(t) = \sum_{j=0}^{2n} B_j u_s(t - t_j) \tag{6}$$

where B_j is the magnitude of a unit step function $u_s(t)$ at t_j. This function can be characterized by its switch pattern as:

$$B = \{ B_0, \quad B_1, \quad B_2, \cdots, B_{2n} \}$$
$$T = \{ t_0, \quad t_1, \quad t_2, \cdots, t_{2n} \}$$

where B represents a set of B_j with $B_0 = B_{2n} = \pm 1$ and $B_j = \pm 2$ for $j = 1, \cdots, 2n-1$; T represents a set of switching times $(t_1, \cdots, t_{2n-1})$ and the initial and final times ($t_0 = 0$ and $t_f = t_{2n}$).

The rest-to-rest maneuvering constraint for the rigid-body mode ($\omega_1 = 0$) can be found as

$$\frac{\phi_1}{2} \sum_{j=0}^{2n} (t_f - t_j)^2 B_j - y_1(t_f) = 0 \tag{7}$$

The i^{th} structural mode solution for the control input of Eq. (6) for $t \geq t_f$ is

$$\begin{aligned} y_i(t) = & -\frac{\phi_i}{\omega_i^2} \sum_{j=0}^{2n} B_j \cos \omega_i (t - t_j) \\ = & -\frac{\phi_i}{\omega_i^2} [\cos \omega_i (t - t_n) \sum_{j=0}^{2n} B_j \cos \omega_i (t_j - t_n) \\ & + \sin \omega_i (t - t_n) \sum_{j=0}^{2n} B_j \sin \omega_i (t_j - t_n)] \end{aligned} \tag{8}$$

and it can be shown that the following constraint equation for each mode

$$\sum_{j=0}^{2n} B_j \sin \omega_i (t_j - t_n) = 0 \tag{9}$$

is always satisfied for any bang-bang input which is symmetric about the mid-maneuver time t_n. Consequently, we have the following flexible mode constraints for no-residual structural vibration (i.e., $y_i(t) = 0$ for $t \geq t_f$):

$$\sum_{j=0}^{2n} B_j \cos \omega_i (t_j - t_n) = 0 \tag{10}$$

for each flexible mode.

On the other hand, for Case 2 with the pulse sequences as illustrated in Fig. 2, the boundary conditions of the rest-to-rest maneuvering problem result in the following constraint:

$$\phi_{11} \sum_{j=0,2}^{N-1} \Delta_j - \phi_{12} \sum_{j=1,3}^{N} \Delta_j = 0 \tag{11}$$

where ϕ_{11} and ϕ_{12} are the modal input distribution coefficients associated with the rigid-body mode and the two control inputs u_1 and u_2, and Δ_j and N are defined as in Fig. 2.

The positioning constraint for the rigid-body mode, with specified $y_1(t \geq t_f)$, then becomes

$$\begin{aligned} & 2y_1(t_f) - \phi_{11} \sum_{j=0,2}^{N-1} [2t_j \Delta_j - \Delta_j] \\ & + \phi_{12} \sum_{j=1,3}^{N} [2t_j \Delta_j - \Delta_j] = 0 \end{aligned} \tag{12}$$

Also, rest-to-rest maneuvering requires that for each flexible mode, $y_i(t) = 0$ for $t \geq t_f$;

i.e., we have

$$-\phi_{i1}\sum_{j=0,2}^{N-1} c_{ij} + \phi_{i2}\sum_{j=1,3}^{N} c_{ij} = 0 \tag{13a}$$

$$\phi_{i1}\sum_{j=0,2}^{N-1} s_{ij} - \phi_{i2}\sum_{j=1,3}^{N} s_{ij} = 0 \tag{13b}$$

where

$$c_{ij} = \cos(\omega_i t_j) - \cos(\omega_i(t_j + \Delta_j))$$
$$s_{ij} = \sin(\omega_i t_j) - \sin(\omega_i(t_j + \Delta_j))$$

for $i = 2, \cdots, n$.

Remark: For cases in which the control inputs are one-sided, each control input for the time-optimal solution need not be an odd function about the mid-maneuver time. Thus, the problem with one-sided control inputs becomes more difficult to solve than the standard problem with two-sided control inputs, and many theoretical issues (e.g., the uniqueness and structure of time-optimal solutions) need to be resolved.

We now present a detailed solution of each case.

Case 1 with a Two-Sided Control Input

In this case, as illustrated in Fig. 1, a two-sided control input is bounded as:

$$-1 \leq u(t) \leq +1$$

and the equations of motion for this case are

$$m_1\ddot{x}_1 + k_1(x_1 - x_2) = u$$
$$m_2\ddot{x}_2 + k_1(x_2 - x_1) + k_2(x_2 - x_3) = 0$$
$$m_3\ddot{x}_3 + k_2(x_3 - x_2) = 0$$

where x_1, x_2 and x_3 are the positions of body 1, body 2 and body 3, respectively, and the nominal parameters are $m_1 = m_2 = m_3 = k_1 = k_2 = 1$ with appropriate units, and time is in units of second.

The boundary conditions for a rest-to-rest maneuver are given as

$$x_1(0) = x_2(0) = x_3(0) = 0 \tag{14a}$$

$$x_1(t_f) = x_2(t_f) = x_3(t_f) = 1 \tag{14b}$$

$$\dot{x}_1(0) = \dot{x}_2(0) = \dot{x}_3(0) = 0 \tag{14c}$$

$$\dot{x}_1(t_f) = \dot{x}_2(t_f) = \dot{x}_3(t_f) = 0 \tag{14d}$$

The modal equations are

$$\ddot{y}_1 = 0.3333u \tag{15a}$$

$$\ddot{y}_2 + \omega_2^2 y_2 = 0.5u \tag{15b}$$

$$\ddot{y}_3 + \omega_3^2 y_3 = -0.1667u \tag{15c}$$

where

$$\omega_2^2 = [-b - \sqrt{b^2 - 4k_1k_2c}]/2 \tag{16a}$$

$$\omega_3^2 = [-b + \sqrt{b^2 - 4k_1k_2c}]/2 \tag{16b}$$

$$b = \frac{-k_1(m_1 + m_2)m_3 - k_2(m_2 + m_3)m_1}{m_1m_2m_3} \tag{16c}$$

$$c = (m_1 + m_2 + m_3)/(m_1m_2m_3) \tag{16d}$$

and $\omega_2 = 1$ rad/sec and $\omega_3 = \sqrt{3}$ rad/sec for the nominal system. The corresponding boundary conditions for the modal coordinates are

$$y_1(0) = y_2(0) = y_3(0) = 0 \tag{17a}$$

$$y_1(t_f) = 1, \quad y_2(t_f) = y_3(t_f) = 0 \tag{17b}$$

$$\dot{y}_1(0) = \dot{y}_2(0) = \dot{y}_3(0) = 0 \tag{17c}$$

$$\dot{y}_1(t_f) = \dot{y}_2(t_f) = \dot{y}_3(t_f) = 0 \tag{17d}$$

The time-optimal control input with 5 switchs is expressed as

$$\begin{aligned} u(t) = {} & u_s(t) - 2u_s(t - t_1) + 2u_s(t - t_2) - 2u_s(t - t_3) \\ & + u_s(t - t_4) - u_s(t - t_5) + u_s(t - t_6) \end{aligned} \tag{18}$$

with the symmetry conditions

$$t_6 = 2t_3$$
$$t_5 = 2t_3 - t_1$$
$$t_4 = 2t_3 - t_2$$

The time-optimal control problem is then formulated as the following constrained minimization problem:

$$min\ J = t_f = t_6 = 2t_3 \tag{19}$$

subject to the following constraints:

$$6 - t_6^2 + \sum_{j=1}^{5}(-1)^{j+1}[2(t_6 - t_j)^2] = 0 \tag{20}$$

$$1 + \cos(\omega_2 t_3) + 2\sum_{j=1}^{2}(-1)^j \cos(\omega_2(t_3 - t_j)) = 0 \tag{21}$$

$$1 + \cos(\omega_3 t_3) + 2\sum_{j=1}^{2}(-1)^j \cos(\omega_3(t_3 - t_j)) = 0 \tag{22}$$

$$t_1,\ t_2,\ t_3 > 0 \tag{23}$$

A standard IMSL FORTRAN subroutine was used to obtain a solution as:

$$\begin{aligned} u(t) = {} & u_s(t) - 2u_s(t - 0.944) + 2u_s(t - 2.012) \\ & - 2u_s(t - 3.255) + u_s(t - 4.499) \\ & - u_s(t - 5.567) + u_s(t - 6.511) \end{aligned} \tag{24}$$

The time responses of x_3 to this time-optimal control input are shown in Fig. 3 for four different values of $k = k_1 = k_2$. We notice that the responses are quite sensitive to variations in the model parameters. Similar responses can also be observed for arbitrarily combined variations of k_i and m_i, but keeping the total mass constant ($m_1+m_2+m_3 = 3$). For convenience, simulation results only for $k = k_1 = k_2$ variations are presented in this paper.

Case 2 with Two One-Sided Control Inputs

For Case 2, as illustrated in Fig. 1, two one-sided control inputs are bounded as

$$0 \le u_1 \le +1 \tag{25a}$$

$$-1 \leq u_2 \leq 0 \tag{25b}$$

For this case, the time-optimal control inputs are assumed as:

$$\begin{aligned} u_1 &= u_s(t) - u_s(t-\Delta_0) \\ &\quad + u_s(t-t_2) - u_s(t-t_2-\Delta_2) \end{aligned} \tag{26a}$$

$$\begin{aligned} u_2 &= -u_s(t-t_1) + u_s(t-t_1-\Delta_1) \\ &\quad - u_s(t-t_3) + u_s(t-t_3-\Delta_3) \end{aligned} \tag{26b}$$

The modal equations for this case are

$$\ddot{y}_1 = 0.3333u_1 + 0.3333u_2 \tag{27a}$$

$$\ddot{y}_2 + \omega_2^2 y_2 = 0.5u_1 \tag{27b}$$

$$\ddot{y}_3 + \omega_3^2 y_3 = 0.1667u_1 - 0.3333u_2 \tag{27c}$$

and the rest-to-rest maneuver constraints are

$$\Delta_0 - \Delta_1 + \Delta_2 - \Delta_3 = 0 \tag{28a}$$

$$6 + \sum_{j=0}^{3}(-1)^j[\Delta_j^2 - 2t_j\Delta_j] = 0 \tag{28b}$$

$$\sum_{j=1,3}[\cos(\omega_2 t_j) - \cos(\omega_2(t_j+\Delta_j))] = 0 \tag{28c}$$

$$\sum_{j=1,3}[\sin(\omega_2 t_j) - \sin(\omega_2(t_j+\Delta_j))] = 0 \tag{28d}$$

$$\begin{aligned} &\sum_{j=1,3}[\cos(\omega_3 t_j) - \cos(\omega_3(t_j+\Delta_j))] \\ &+ 2\sum_{j=0,2}[\cos(\omega_3 t_j) - \cos(\omega_3(t_j+\Delta_j))] = 0 \end{aligned} \tag{28e}$$

$$\begin{aligned} &\sum_{j=1,3}[\sin(\omega_3 t_j) - \sin(\omega_3(t_j+\Delta_j))] \\ &+ 2\sum_{j=0,2}[\sin(\omega_3 t_j) - \sin(\omega_3(t_j+\Delta_j))] = 0 \end{aligned} \tag{28f}$$

The time-optimal solution can then be obtained by solving the constrained minimization problem:

$$min\ J = t_f = t_3 + \Delta_3 \tag{29}$$

subject to the constraint given by Eqs. (28).

A solution of this problem can be found as

$$\begin{array}{ll} t_0 = 0.0000, & \Delta_0 = 0.8459 \\ t_1 = 1.1594, & \Delta_1 = 1.0487 \\ t_2 = 2.1455, & \Delta_2 = 1.2516 \\ t_3 = 4.3010, & \Delta_3 = 1.0487 \\ t_f = 5.3497 & \end{array} \tag{30}$$

The time responses of x_3 to the time-optimal control inputs are shown in Fig. 4 for four different values of $k = k_1 = k_2$. Similar to Case 1, the responses are sensitive to variations in the model parameters. An interesting feature of this case is that the pulse sequences are of a "bang-off-bang" type, resulting in the control on-time of 4.195 sec, which is different from the maneuver time of 5.35 sec.

Case 3 with Two One-Sided Control Inputs

For Case 3, as illustrated in Fig. 1, two one-sided control inputs are bounded as

$$0 \leq u_1 \leq +1 \tag{31a}$$

$$-1 \leq u_3 \leq 0 \tag{31b}$$

Similar to Case 2, the time-optimal control inputs are assumed as:

$$\begin{aligned} u_1 = {} & u_s(t) - u_s(t - \Delta_0) \\ & + u_s(t - t_2) - u_s(t - t_2 - \Delta_2) \end{aligned} \tag{32a}$$

$$\begin{aligned} u_3 = {} & -u_s(t - t_1) + u_s(t - t_1 - \Delta_1) \\ & - u_s(t - t_3) + u_s(t - t_3 - \Delta_3) \end{aligned} \tag{32b}$$

The modal equations for this case are

$$\ddot{y}_1 = 0.3333(u_1 + u_3) \tag{33a}$$

$$\ddot{y}_2 + \omega_2^2 y_2 = 0.5(u_1 - u_3) \tag{33b}$$

$$\ddot{y}_3 + \omega_3^2 y_3 = 0.1667(u_1 + u_3) \tag{33c}$$

and the rest-to-rest maneuver constraints are

$$\Delta_0 - \Delta_1 + \Delta_2 - \Delta_3 = 0 \tag{34a}$$

$$6 + \sum_{j=0}^{3}(-1)^j[\Delta_j^2 - 2t_j\Delta_j] = 0 \tag{34b}$$

$$\sum_{j=0}^{3}(-1)^j[\sin(\omega_2 t_j) - \sin(\omega_2(t_j + \Delta_j))] = 0 \tag{34c}$$

$$\sum_{j=0}^{3}(-1)^j[\cos(\omega_2 t_j) - \cos(\omega_2(t_j + \Delta_j))] = 0 \tag{34d}$$

$$\sum_{j=0}^{3}(-1)^j[\sin(\omega_3 t_j) - \sin(\omega_3(t_j + \Delta_j))] = 0 \tag{34e}$$

$$\sum_{j=0}^{3}(-1)^j[\cos(\omega_3 t_j) - \cos(\omega_3(t_j + \Delta_j))] = 0 \tag{34f}$$

$$t_1, t_2, t_3, t_4, t_5 > 0; \quad t_0 = 0$$

$$\Delta_j \geq 0$$

The time-optimal solution can then be obtained by solving the constrained minimization problem:

$$min\ J = t_f = t_3 + \Delta_3 \tag{35}$$

subject to the constraints given by Eqs. (34).

A solution of this problem is

$$\begin{array}{ll} t_0 = 0.0000, & \Delta_0 = 0.9510 \\ t_1 = 1.3631, & \Delta_1 = 0.1658 \\ t_2 = 2.8329, & \Delta_2 = 0.1658 \\ t_3 = 3.4109, & \Delta_3 = 0.9510 \\ t_f = 4.3619 & \end{array} \tag{36}$$

The time responses of x_3 to the time-optimal control inputs are shown in Fig. 5 for four different values of $k = k_1 = k_2$. Again, the responses are quite sensitive to variations in the model parameters. Similar to Case 2, an interesting feature of this case is that the pulse sequences are of a "bang-off-bang" type, resulting in the control on-time of 2.234 sec, which is different from the maneuver time of 4.362 sec.

Compared to Case 1 and Case 2, this case has the fastest maneuver time as well as the smallest control on-time. Therefore, the actuator configuration of Case 3 can be considered to be "optimal" in the sense of minimizing both the maneuver time and the jet on-time.

3. Robust Time-Optimal Control

As shown in the preceding section, a standard, time-optimal control approach requires an accurate mathematical model and thus the resulting solution is often sensitive to plant modeling uncertainty.

In this section, expanding on the approach introduced in Section 2, a parameter optimization problem is formulated with additional constraints for robustness with respect to the structural frequency uncertainty. The resulting *robustified* or *desensitized*, time-optimal soultion is a multi-switch bang-bang control, and is thus implementable for spacecraft equipped with on-off reaction jets [3].

Problem Formulation

By taking the derivative of Eq. (8) with respect to ω_i, we get

$$\frac{dy_i(t)}{d\omega_i} = \frac{\phi_i}{\omega_i^2}\cos\omega_i(t-\frac{t_f}{2})\sum_{j=0}^{2n}(t_j-\frac{t_f}{2})B_j\sin\omega_i(t_j-\frac{t_f}{2}) \tag{37}$$

for each flexible mode. Letting $dy_i(t)/d\omega_i = 0$ for all $t \geq t_f$, we have

$$\sum_{j=0}^{2n}(t_j-\frac{t_f}{2})B_j\cos\omega_i(t_j-\frac{t_f}{2}) = 0;\ i = 2,\cdots,n \tag{38}$$

which are called the first-order robustness constraints for the case with a two-sided control input.

Similarly, the robustness constraints for a case with two one-sided control inputs can be found as:

$$-\phi_{i1}\sum_{j=0,2}^{N-1}c_{ij} + \phi_{i2}\sum_{j=1,3}^{N}c_{ij} = 0 \tag{39a}$$

$$\phi_{i1}\sum_{j=0,2}^{N-1}s_{ij} - \phi_{i2}\sum_{j=1,3}^{N}s_{ij} = 0 \tag{39b}$$

where

$$c_{ij} = t_j\cos(\omega_i t_j) - (t_j+\Delta_j)\cos(\omega_i(t_j+\Delta_j))$$

$$s_{ij} = t_j\sin(\omega_i t_j) - (t_j+\Delta_j)\sin(\omega_i(t_j+\Delta_j))$$

which are called the first-order robustness constraints for the case with two one-sided control inputs.

Case 1 with a Two-Sided Control Input

For Case 1, the time-optimal control is a five-switch bang-bang function, but the resulting responses were shown to be very sensitive to variations in model parameters. A robustified, time-optimal solution of the same problem is now computed as follows. The robust time-optimal control input is assumed as:

$$u(t) = u_s(t) + 2\sum_{j=1}^{9}[(-1)^j u_s(t - t_j)] + u_s(t - t_{10}) \tag{40}$$

with the symmetry conditions

$$\begin{aligned} t_6 &= 2t_5 - t_4 \\ t_7 &= 2t_5 - t_3 \\ t_8 &= 2t_5 - t_2 \\ t_9 &= 2t_5 - t_1 \\ t_{10} &= 2t_5 \end{aligned} \tag{41}$$

The constrained optimization problem with the first-order robustness constraint can be formulated as:

$$min\ J = t_f = t_{10} \tag{42}$$

subject to

$$6 + \sum_{j=1}^{9}(-1)^{j+1}[2(t_{10} - t_j)^2] - t_{10}^2 = 0$$

$$1 + \cos(\omega_2 t_5) + 2\sum_{j=1}^{4}[(-1)^j \cos(\omega_2(t_j - t_5))] = 0$$

$$1 + \cos(\omega_3 t_5) + 2\sum_{j=1}^{4}[(-1)^j \cos(\omega_3(t_j - t_5))] = 0$$

$$t_5 \sin(\omega_2 t_5) + 2\sum_{j=1}^{4}(-1)^j(t_j - t_5)\sin(\omega_2(t_j - t_5)) = 0$$

$$t_5 \sin(\omega_3 t_5) + 2\sum_{j=1}^{4}(-1)^j(t_j - t_5)\sin(\omega_3(t_j - t_5)) = 0$$

$$t_1, t_2, t_3, t_4, t_5 > 0; \quad t_0 = 0$$

A robust time-optimal solution with 9 switches can be found as:

$$\begin{aligned} t_1 &= 0.560, \quad t_2 = 1.460 \\ t_3 &= 2.690, \quad t_4 = 3.804 \\ t_5 &= 5.091, \quad t_6 = 6.377 \\ t_7 &= 7.491, \quad t_8 = 8.722 \\ t_9 &= 9.622, \quad t_{10} = 10.18 \end{aligned} \tag{43}$$

The time responses of x_3 to this robust time-optimal control input are shown in Fig. 6 for four different values of $k = k_1 = k_2$. We notice that the resulting responses are less sensitive to parameter variations, as compared to the responses to the ideal, time-optimal control input, as shown in Fig. 3. The second flexible mode is significantly excited during manuevers, however. Performance robustness has been increased at the expense of the increased maneuvering time of 10.18 sec, as compared to the ideal minimum-time of 6.511 sec. It is, however, emphasized that simply prolonging the maneuver time does not help to reduce residual structural vibrations caused by modeling uncertainty; a proper pulse sequence is necessary.

Case 2 with Two One-Sided Control Inputs

For Case 2, we can represent the control inputs as follows:

$$\begin{aligned} u_1 &= u_s(t) - u_s(t-\Delta_0) + u_s(t-t_2) \\ &\quad - u_s(t-t_2-\Delta_2) + u_s(t-t_4) - u_s(t-t_4-\Delta_4) \\ u_2 &= -u_s(t-t_1) + u_s(t-t_1-\Delta_1) - u_s(t-t_3) \\ &\quad + u_s(t-t_3-\Delta_3) - u_s(t-t_5) + u_s(t-t_5-\Delta_5) \end{aligned}$$

where we have 11 unknowns to be determined, and t_j and Δ_j are defined as in Fig. 2.

The robust time-optimal solution can then be obtained by solving the constrained parameter optimization problem

$$min\ J = t_f = t_5 + \Delta_5 \tag{44}$$

subject to

$$\Delta_0 - \Delta_1 + \Delta_2 - \Delta_3 + \Delta_4 - \Delta_5 = 0$$

$$
\begin{aligned}
&6+\sum_{j=0}^{5}(-1)^j[\Delta_j^2-2t_j\Delta_j]=0\\
&\sum_{j=1,3}[\cos(\omega_2 t_j)-\cos(\omega_2(t_j+\Delta_j))]=0\\
&\sum_{j=1,3}[\sin(\omega_2 t_j)-\sin(\omega_2(t_j+\Delta_j))]=0\\
&\sum_{j=1,3}[\cos(\omega_3 t_j)-\cos(\omega_3(t_j+\Delta_j))]\\
&+2\sum_{j=0,2,4}[\cos(\omega_3 t_j)-\cos(\omega_3(t_j+\Delta_j))]=0\\
&\sum_{j=1,3}[\sin(\omega_3 t_j)-\sin(\omega_3(t_j+\Delta_j))]\\
&+2\sum_{j=0,2,4}[\sin(\omega_3 t_j)-\sin(\omega_3(t_j+\Delta_j))]=0\\
&\sum_{j=1,3}[t_j\cos(\omega_2 t_j)-(t_j+\Delta_j)\cos(\omega_2(t_j+\Delta_j))]=0\\
&\sum_{j=1,3}[t_j\sin(\omega_2 t_j)-(t_j+\Delta_j)\sin(\omega_2(t_j+\Delta_j))]=0\\
&\sum_{j=1,3}[t_j\cos(\omega_3 t_j)-(t_j+\Delta_j)\cos(\omega_3(t_j+\Delta_j))]\\
&+2\sum_{j=0,2,4}[t_j\cos(\omega_3 t_j)-(t_j+\Delta_j)\cos(\omega_3(t_j+\Delta_j))]=0\\
&\sum_{j=1,3}[t_j\sin(\omega_3 t_j)-(t_j+\Delta_j)\sin(\omega_3(t_j+\Delta_j))]\\
&+2\sum_{j=0,2,4}[t_j\sin(\omega_3 t_j)-(t_j+\Delta_j)\sin(\omega_3(t_j+\Delta_j))]=0\\
&\Delta_j\geq 0;\quad j=0,1,2,3,4,5\\
&t_1,\ t_2,\ t_3,\ t_4,\ t_5>0\ ;\ t_0=0
\end{aligned}
$$

A solution to this problem is:

$$
\begin{aligned}
t_0&=0.0000, & \Delta_0&=0.3855\\
t_1&=0.4440, & \Delta_1&=0.5783\\
t_2&=1.6118, & \Delta_2&=1.4181\\
t_3&=3.2990, & \Delta_3&=1.2131\\
t_4&=4.8208, & \Delta_4&=0.5661\\
t_5&=6.7887, & \Delta_5&=0.5783\\
t_f&=7.3671
\end{aligned}
\qquad (45)
$$

The time responses of x_3 to the robust time-optimal control inputs are shown in Fig. 7 for four different values of $k=k_1=k_2$. Similar to Case 1 of the preceding section,

the robustness has been increased at the expense of the increased maneuvering time of 7.367 sec, as compared to the ideal minimum-time of 5.35 sec. The jet on-time is 4.195 sec. The second flexible mode is less excited, as compared to Case 1.

Case 3 with Two One-Sided Control Inputs

Assuming that each control input has two pulses as in Case 2, we can represent the control inputs as:

$$\begin{aligned} u_1 &= u_s(t) - u_s(t-\Delta_0) + u_s(t-t_2) - u_s(t-t_2-\Delta_2) \\ &\quad + u_s(t-t_4) - u_s(t-t_4-\Delta_4) \\ u_3 &= -u_s(t-t_1) + u_s(t-t_1-\Delta_1) - u_s(t-t_3) \\ &\quad + u_s(t-t_3-\Delta_3) - u_s(t-t_5) + u_s(t-t_5-\Delta_5) \end{aligned}$$

where we have 11 unknowns to be determined, and t_j and Δ_j are defined as in Fig. 2.

The robust time-optimal solution can then be obtained by solving the constrained parameter optimization problem

$$min\ J = t_5 + \Delta_5 \tag{47}$$

subject to

$$\Delta_0 - \Delta_1 + \Delta_2 - \Delta_3 + \Delta_4 - \Delta_5 = 0$$

$$6 + \sum_{j=0}^{5}(-1)^j[\Delta_j^2 - 2t_j\Delta_j] = 0$$

$$\sum_{j=0}^{5}(-1)^j[\sin(\omega_2 t_j) - \sin(\omega_2(t_j+\Delta_j))] = 0$$

$$\sum_{j=0}^{5}(-1)^j[\cos(\omega_2 t_j) - \cos(\omega_2(t_j+\Delta_j))] = 0$$

$$\sum_{j=0}^{5}[(-1)^j\sin(\omega_3 t_j) - \sin(\omega_3(t_j+\Delta_j))] = 0$$

$$\sum_{j=0}^{5}[(-1)^j\cos(\omega_3 t_j) - \cos(\omega_3(t_j+\Delta_j))] = 0$$

$$\sum_{j=0}^{5}(-1)^j[t_j\cos\omega_2 t_j - (t_j+\Delta_j)\cos\omega_2(t_j+\Delta_j)] = 0$$

$$\sum_{j=0}^{5}(-1)^j[t_j \sin\omega_2 t_j - (t_j+\Delta_j)\sin\omega_2(t_j+\Delta_j)] = 0$$

$$\sum_{j=0}^{5}(-1)^j[t_j \cos\omega_3 t_j - (t_j+\Delta_j)\cos\omega_3(t_j+\Delta_j)] = 0$$

$$\sum_{j=0}^{5}(-1)^j[t_j \sin\omega_3 t_j - (t_j+\Delta_j)\sin\omega_3(t_j+\Delta_j)] = 0$$

$$\Delta_j \geq 0; \quad j = 0,1,2,3,4,5$$

$$t_1,\ t_2,\ t_3,\ t_4,\ t_5 > 0;\ \ t_0 = 0$$

A solution to this problem is

$$\begin{aligned} t_0 &= 0.000, \quad \Delta_0 = 0.2189 \\ t_1 &= 3.774, \quad \Delta_1 = 0.2609 \\ t_2 &= 2.030, \quad \Delta_2 = 0.3594 \\ t_3 &= 5.778, \quad \Delta_3 = 0.3594 \\ t_4 &= 4.152, \quad \Delta_4 = 0.2609 \\ t_5 &= 7.968, \quad \Delta_5 = 0.2189 \\ t_f &= 8.187 \end{aligned} \tag{48}$$

The time responses of x_3 to the robust time-optimal control inputs are shown in Fig. 8 for four different values of $k = k_1 = k_2$. The robustness has been increased at the expense of the increased maneuvering time of 8.187 sec, as compared to the ideal minimum-time of 4.362 sec. However, the control on-time is only *1.678 seconds!* Because of the properly coordinated pulse sequences, the flexible modes are not significantly excited during manuevers and the residual responses after the maneuvers are well desensitized.

4. Summary

In this paper, we have demonstrated that the proposed *robustification* or *desensitization* approach does generate *robust* time-optimal open-loop control inputs for uncertain dynamical systems. Furthermore, on the contrary to a common notion, the results of this paper indicate that properly coordinated, on-off pulse sequences can achieve a fast maneuvering time with a minimum of structural vibrations during and/or after a maneuver, even in the face of plant modeling uncertainty. The time-optimal responses have been desensitized at the expense of the increased maneuvering time. It is again emphasized that simply prolonging the maneuver time does not help to reduce residual

structural vibrations caused by modeling uncertainty; a proper coordination of pulse sequences is necessary, as demonstrated in this paper.

The results of this paper are summarized in Table 1. As can be noticed in this table, it is natural to select the actuator configuration of Case 3, since this case provides the "best" overall performance in the sense of minimizing the maneuvering time, fuel consumption (jet on-time), and structural mode excitation. For Case 1, the maneuvering time and the jet on-time are the same, which is clearly undesirable from the viewpoint of fuel consumption. To avoid such undesirable continuous jet firings during a maneuver, a robust fuel- and time-optimal control problem is formulated in [4].

5. Conclusions

A time-optimal open-loop control problem of flexible spacecraft in the face of modeling uncertainty has been investigated. The primary study objective was to explore the feasibility of computing open-loop, on-off pulse control logic for uncertain flexible spacecraft. The results indicate that the proposed approach significantly reduces the residual structural vibrations caused by modeling uncertainty. The results also indicate the importance of a proper jet placement for practical trade-offs among the maneuvering time, fuel consumption, and performance robustness.

Acknowledgments

This research was supported by the NASA Johnson Space Center through the RICIS program of the University of Houston at Clear Lake. The authors would like to express special thanks to Dr. Kenneth Cox and Dr. John Sunkel of the NASA JSC for sponsoring this research.

References

[1] B. Wie and Q. Liu, "A Comparison Between Robustified Feedforward and Feedback for Achieving Performance Robustness," Proceedings of AIAA GN&C Conference, August 20-22, 1990, to appear in the *Journal of Guidance, Control and Dynamics.*

[2] Q. Liu and B. Wie, "Robust Time-Optimal Control of Uncertain Flexible Spacecraft," Proceedings of AIAA GN&C Conference, August 12-14, 1991, to appear in the *Journal of Guidance, Control and Dynamics.*

[3] T.C. Anthony, B. Wie and S. Carroll, "Pulse Modulated Control Synthesis for a Flexible Spacecraft," *Journal of Guidance, Control and Dynamics*, Vol. 13, No.'6, 1990, pp.1014–1022.

[4] B. Wie, R. Sinha and Q. Liu, "Robust Fuel- and Time-Optimal Control of Flexible Spacecraft," to be presented at the 1992 *IEEE Conference on Decision and Control*, December 16-18, 1992.

Table 1: Summary of the results

Time-Optimal Control		
	$J^* = t_f$(sec)	Jet On-Time
Case 1	6.511	6.511
Case 2	5.350	4.195
Case 3	4.362	2.234
Robust Time-Optimal Control		
	$J^* = t_f$(sec)	Jet On-Time
Case 1	10.18	10.18
Case 2	7.367	4.739
Case 3	8.187	1.678

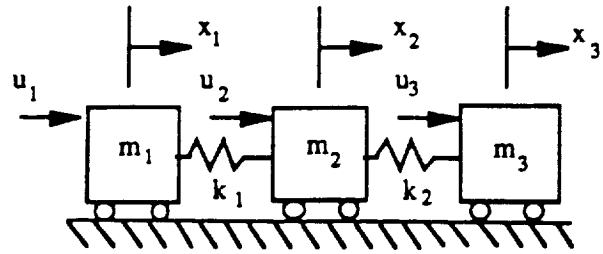

Case #1: $|u_1| \le 1$, $u_2 = 0$, $u_3 = 0$

Case #2: $0 \le u_1 \le +1$, $-1 \le u_2 \le 0$, $u_3 = 0$

Case #3: $0 \le u_1 \le +1$, $u_2 = 0$, $-1 \le u_3 \le 0$

Figure 1: Three-mass-spring dynamical system.

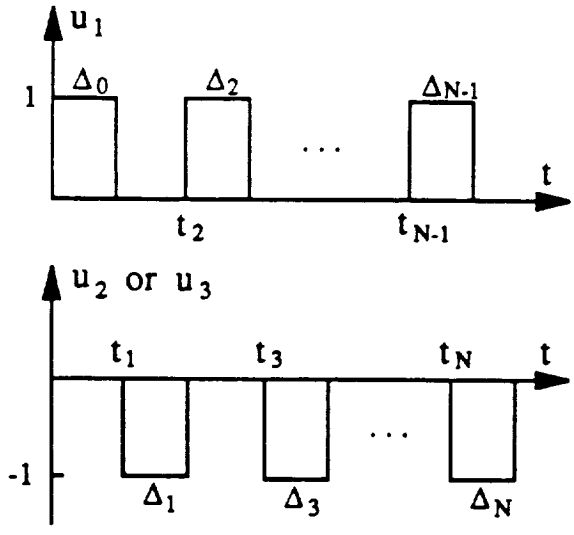

Figure 2: Pulse sequences.

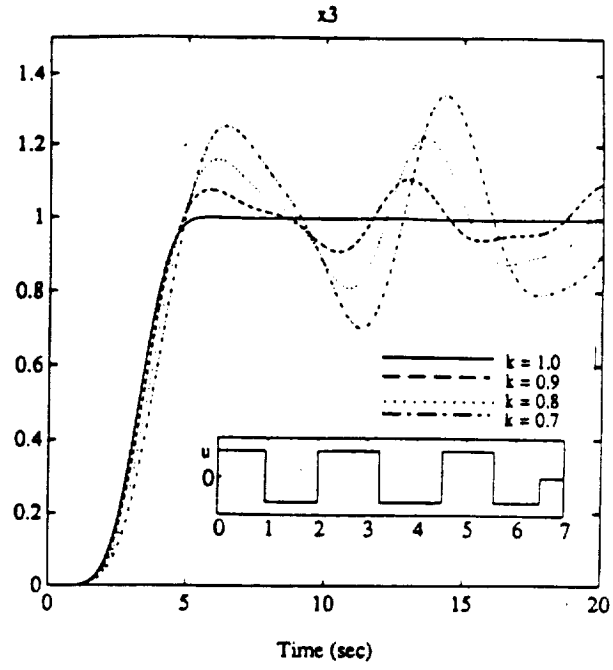

Figure 3: Responses of time-optimal control Case 1.

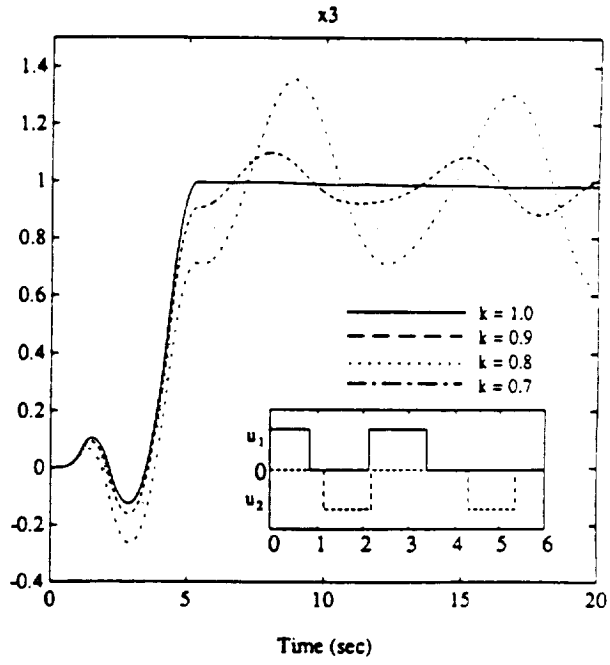

Figure 4: Responses of time-optimal control Case 2.

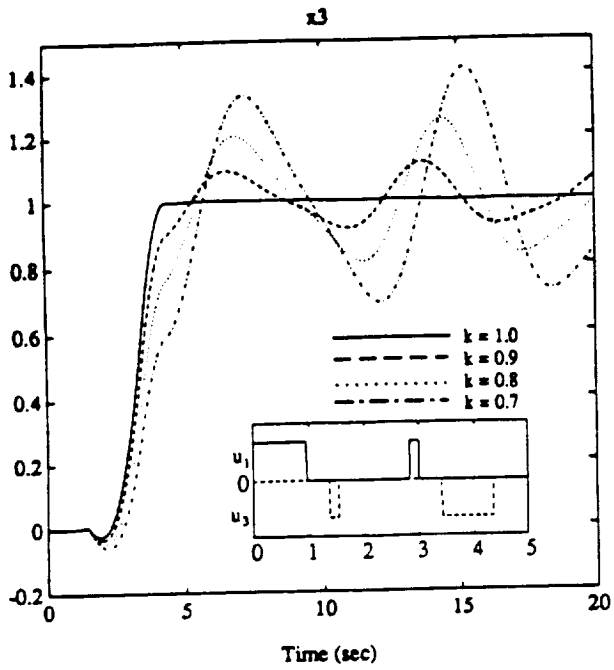

Figure 5: Responses of time-optimal control Case 3.

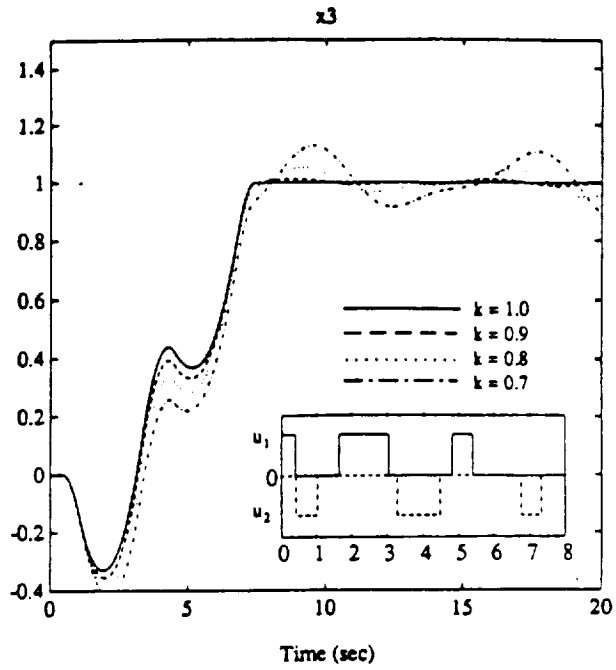

Figure 7: Responses of robust time-optimal control Case 2.

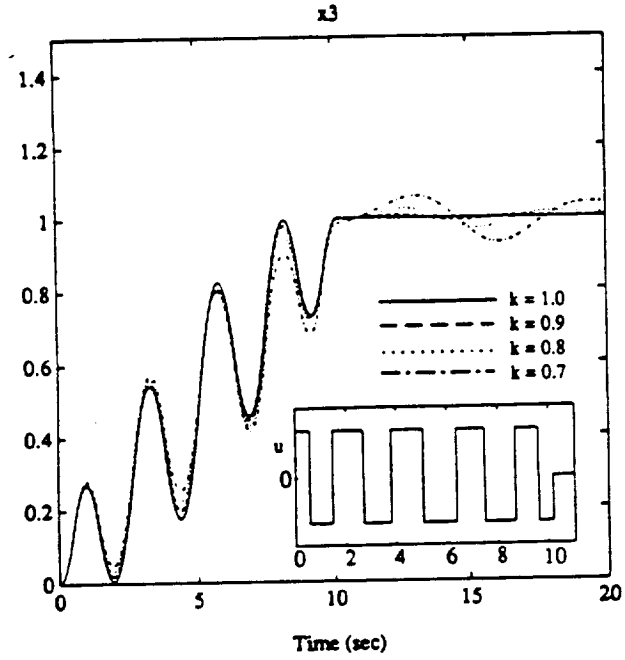

Figure 6: Responses of robust time-optimal control Case 1.

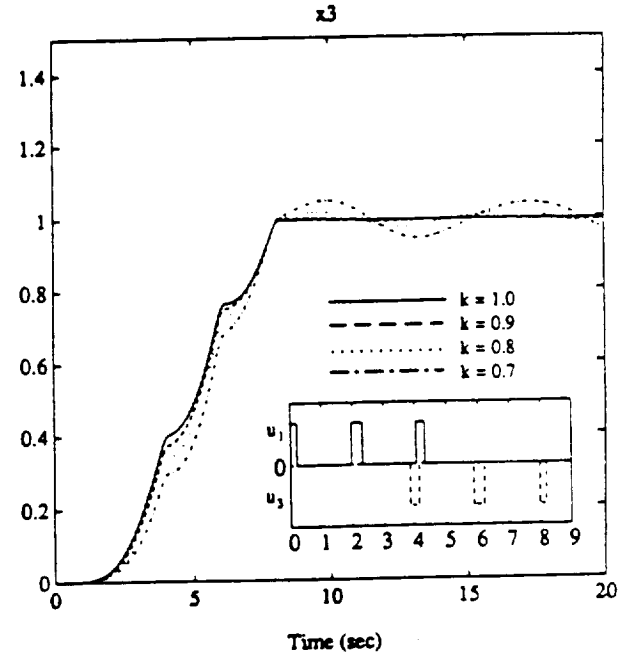

Figure 8: Responses of robust time-optimal control Case 3.

Copies of this publication have been deposited with the Texas State Library in compliance with the State Depository Law.